ARE PCBS IN PHYTOPLANKTON AND ZOOPLANKTON AT EQUILIBRIUM WITH THE WATER IN WHICH THEY LIVE?

by

Angela Cacciola
B.A., Chemistry, Barnard College, 2015

Submitted to the department of Civil and Environmental Engineering
in partial fulfillment of the requirements for the degree of Master of Science at the
MASSACHUSETTS INSTITUTE OF TECHNOLOGY
September 2019

Signature of author   **Signature redacted**

_____
O Angela Cacciola
                Department of Civil and Environmental Engineering, MIT

                        Signature redacted

Certified by

_____
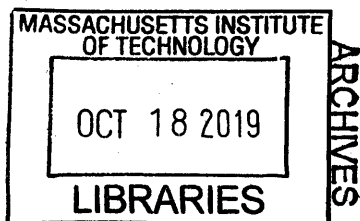   Philip M. Gschwend
        Ford Professor of Civil and Environmental Engineering
                                    Thesis supervisor, MIT

Accepted by   **Signature redacted**

_____
                                      Colette Heald
        Professor of Civil and Environmental Engineering
                Chair, Graduate Program Committee, MIT

ARE PCBS IN PHYTOPLANKTON AND ZOOPLANKTON AT EQUILIBRIUM WITH THE WATER IN WHICH THEY LIVE?

by

Angela Cacciola

Submitted to the Department of Civil and Environmental Engineering
on August 27, 2019 in Partial Fulfillment of the Requirements for the
Degree of Master of Science

ABSTRACT

Food chain bioaccumulation of polychlorinated biphenyls (PCBs) can result in harmful concentrations within higher trophic level organisms such as fish and humans. It is important to consider how the concentrations of PCBs in phytoplankton and zooplankton affect higher trophic organisms. It was hypothesized that polychlorinated biphenyl (PCB) concentrations within primary producers such as phytoplankton simply reflect chemical equilibrium of PCB congeners freely dissolved in the water column and in the lipid fraction of the plankton. In this study, the freely dissolved PCBs in the water of Lake Cochituate, MA, were measured using polyethylene (PE) passive sampling strips, thereby avoiding problems associated with colloid-bound PCBs. Phytoplankton and zooplankton samples were measured to determine their PCB levels and lipid fractions. The phytoplankton were at equilibrium in the fall of 2016. The phytoplankton and zooplankton appeared close to equilibrium in the spring of 2017. The large PCB congeners measured in the spring of 2017 may have been undersaturated, consistent with the idea that rapid growth leads to phytoplankton undersaturation.

Thesis supervisor: Philip M. Gschwend
Title: Ford Professor of Civil and Environmental Engineering

Table of Contents

Figures and Tables

List of abbreviations and symbols

CF correction factor

f_{pe} fraction of PRCs in the polyethylene after sampler deployment

f_{lipid} fraction of lipid in the dry total solids

$f_{protein}$ fraction of protein in the dry total solids

HOCs hydrophobic organic chemicals

K_{lw} lipid water partition coefficient

K_{oc} organic carbon water partition coefficient

K_{ow} octanol water partition coefficient

PCBs polychlorinated biphenyls

PE polyethylene

PH phytoplankton

PM particulate matter

POC particulate organic carbon

PON particulate organic nitrogen

PRCs performance reference compounds

RF response factor

TS total solids

ZO zooplankton

4

Introduction

The environmental impact of hydrophobic organic chemicals (HOCs), such as PCBs (polychlorinated biphenyls), is a matter of critical importance to humans and the rest of the ecosystem. PCBs are toxic, bioaccumulative, and persistent in the environment. Although they were banned in the USA in 1979, they remain in lakes and rivers, where they are absorbed by organic material and accumulate in the food web.

Phytoplankton form the base of the aquatic food web, so in order to understand how HOCs affect higher trophic organisms, the chemical concentrations of these contaminants in the phytoplankton must be determined. This is challenging because environmental samples are spatially and temporally heterogenous and depend on a wide variety natural and human factors. Also, many of these chemicals have low solubility in water and are therefore analytically challenging to measure.

In this work, new water passive sampling methods were applied to more accurately measure the truly dissolved concentrations of a range of PCBs in the water of Lake Cochituate in Natick, MA, in Fall 2016 and Spring 2017. Additionally, measurements of the PCB concentrations in phytoplankton and zooplankton from the same lake were made. The phytoplankton and zooplankton samples were also characterized by their fractions of lipid, protein (via nitrogen measures), and organic carbon. Plankton uptake estimates were made from the freely dissolved water concentrations using lipid-water partition coefficients, K_{lw}. The goals were to ascertain if phytoplankton concentrations for a range of PCB congeners were at equilibrium with the water and to provide quality data to assist in the development of food web models.

Previous work

In the past, the main approach used to assess the equilibrium status of phytoplankton was to measure the chemical in whole phytoplankton, normalize the concentration to lipid content, and divide by the chemical concentrations in which the plankton live [40, 33, 39, 7, 51, 6, 34]. This approach assumed that the majority of the chemical body burden associates with the lipid portion. It also required a method to determine the freely dissolved concentrations in the water. The concentrations in the organism divided by the concentrations in the surrounding water were then compared with the octanol-water partition constant, K_{ow}, to evaluate if contaminants in the plankton were equilibrated with the water.

A variety of other studies compared the ratio of concentrations and the phytoplankton and water to the log K_{ow} [34, 38, 39, 39, 41], but none of these studies considered the truly dissolved water concentration. For example, the work of Skoglund and Swackhamer considered the accumulation of PCBs in phytoplankton cultures and field settings [41]. Ultimately, these studies found that the growth status of phytoplankton species affected the equilibrium partitioning. When plankton growth rates were equal in magnitude to PCB partitioning rates, compounds with log $K_{ow} > 6$ were under-equilibrated. Swackhamer et al. measured operationally defined dissolved

concentrations in the water, that is, concentrations that pass through a filter. This is not necessarily equal to the truly dissolved as this type of measurement does not account for the presence of colloid-bound contaminants [23].

Nizetto et al. (2012) normalized phytoplankton concentrations to organic carbon and estimated the dissolved phase of the water from the filtered water concentrations. This required the assumption that there are no colloids. Also relevant is that phytoplankton organic carbon does not necessarily reflect the organic carbon in the sediment. Other studies were plagued by a variety of problems, such as the isolation of sufficient mass of phytoplankton to measure concentrations of low solubility contaminants [50], and comparisons of time variant measurements of water and plankton concentrations [13]. Lastly, many studies suggested that phytoplankton were at equilibrium on the basis that lipid normalized and water concentration normalized phytoplankton concentrations were linearly correlated with K_{ow}. However, if octanol water sufficiently represents the primary sorptive material in phytoplankton (lipid), then at equilibrium the normalized concentrations should be equivalent, not simply linearly related, to K_{ow}.

Log K_{ow} based food web models are used to predict concentrations in organisms when empirical measurements are not available [14, 16, 44]. These models are site specific and therefore require calibration. The main model used to estimate phytoplankton bioaccumulation [5] is based on the data of Swackhamer [41], which may be unreliable for the reasons discussed above (i.e., lack of equilibrium, inaccurate measures of truly dissolved concentrations, inappropriate values of partition coefficients). The Gobas model is the basis for the KABAM (K_{ow} Based Aquatic Bioaccumulation Model), which is used by the Environmental Protection Agency (EPA) to estimate the bioaccumulation potential and associated mammalian risks of HOCs in aquatic food webs for regulation purposes [5, 20, 27].

Low density polyethylene (PE) sampling methods have been developed to measure the truly dissolved concentrations of hydrophobic organic chemicals in the aquatic environment [1, 9, 22, 45]. Samplers are inserted into the environment of interest so that they can absorb contaminants. Mass transfer and equilibrium information is used to correct field measured PE concentrations for disequilibrium and infer freely dissolved water concentrations [4, 18, 35]. In this study, we incorporated these PE sampling methods with phytoplankton and zooplankton measurements to overcome some of the shortcomings of previous work. We also correct for water temperature and phase-specific partitioning in phytoplankton, i.e. considering both lipids and proteins.

6

Materials and Methods

Materials

All samples and extracts were stored and processed in glassware pre-combusted at 450°C for 12h. Plastic vial caps with Teflon inserts were lined with aluminum foil to limit PCB losses to the polymeric teflon. Phytoplankton samples were collected in amber or foil-wrapped bottles due to light-sensitive chlorophyll pigments.

Dichloromethane, hexane, methanol and chloroform solvents used in this study were purchased from VWR (JT Baker Ultra resi-analyzed). A target PCB calibration standard mixture (1 μg/ml, EPA 20 PCB Congener Calibration Check Solution, RPC-EPA2-1 lot CJ-344) was purchased from Ultra Scientific. Injection standard compounds (100 μg/ml in hexane, PCBs-39, 55, 104, 150 and 188) were purchased from Ultra Scientific. 13C-labeled surrogate (40 μg/ml in nonane, ^{13C}PCBs-19, 52, 105, 167 and 170) and performance reference compounds (PRCs, 40 μg/ml in nonane, 13C-PCBs-28, 47, 52, 101, 111, 138 and 178) were purchased from Cambridge Isotope Laboratory (Tewskbury, MA).

1 mil plastic low density polyethylene (PE) sheets were purchased for passive sampling (25.4 μm, Film Guard by Berry Plastics, Evansville, Indiana). A 63 μm mesh phytoplankton net with a weighted cod end belonged to the field work contractors, Normandeau Associates (Sea Gear Model 9000 Plankton Net, 42.5 cm x 114 cm, Melbourne, FL). Mesh lined windows were cut into the cod end to increase water flow. A 150 μm Nitex-mesh zooplankton net and a lined cod-end was purchased from Aquatic Research (Simple model, 30 cm x 90 cm, Hope, ID). At the end of the cod end was a 1.2 kg ballast weight to help the net sink.

Plankton field collection and sample composition analysis

The concentrations of PCBs in phytoplankton were measured in two seasons (Fall 2016 and Spring/Summer 2017) and at two sites per season (Sites 1 and Site 8). Site 1 was chosen for its proximity to a 1980s PCB spill location, while Site 8 was chosen to determine background PCB concentrations. Zooplankton were only collected in late July of 2017. Site locations are shown in Figure 1 below.

Figure 1. South Pond of Lake Cochituate Phytoplankton Sites

Phytoplankton and zooplankton samples in this study are defined as the material collected with either a 63 μm or 150 μm net, respectively. The nets available for sampling were 21 μm, 63 μm and 150 μm. It was expected that a 21 μm net would yield a higher detritus or dissolved organic matter to phytoplankton mass ratio. Typically, the size cut offs for collecting phytoplankton and zooplankton are operationally defined, which is why the classes of organisms collected by net towing often vary in the literature. Especially in 2017, ancillary analyses (microscope observations, chlorophyll, TS, PM, POC, PON, silica content, lipid content, protein content) were made to further characterize sample composition.

Sample naming

In this document, samples are named according to the following indices: year collected (16 or 17), sample material (PH for phytoplankton, ZO for zooplankton, PE for polyethylene), site number (S1 through S10), and sample number (.1, .2, .3, .4, .D or .E) for phytoplankton and sample type for PE with .05 for overlying water and .WC for water column). For example, 17PHS1.2 refers to the second phytoplankton sample collected from site 1 in 2017. Similarly, 17PES1.05 refers to the 0-5 cm polyethylene sample (from the water overlying the sediment) collected at site 1 in 2017.

Phytoplankton 2016

Phytoplankton were collected at Sites 1, 2, 5A and 8 by MIT-JM on November 2, 2016, near the water surface via a boat tow (Normandeau Associates, Hampton, NH). Two samples were collected per site. Each 1-L plankton sample collected was the result 3 to 4 x 1 min, 63 μm net tows at ~1 mph. After each tow, there was a film covering the net and DI water was used to rinse this material into the cod end. The cod end was then emptied into the glass sample jar. The boat was then turned around and the next tow completed over the same area in the opposite direction. According to these tow specifications, samples were concentrated about 65-90 times (= volume in cod end jar divided by the net opening area times the distance traveled). Samples were stored on ice until they were brought back to the lab in the late afternoon.

The TS (total solids) in the samples were measured to estimate the dry mass of the samples. 50 ml of hand-shaken phytoplankton samples were pipetted into ~2g tared aluminum tins and weighed. The boats were foil covered and placed in a 60°C oven until dry and then re-weighed. Density was calculated from the wet mass and volume. TS was calculated as the ratio of dry solids mass to volume of water subsampled. The DOC (OC mass from GFF filtrate/volume plankton sample) was measured by high temperature oxidation with a Shimadzu TOC-5000 carbon analyzer [32].

The lipid contents of 16PH8 were measured independently of the PCBs but via the same extraction procedure. 100 ml were extracted with DCM (detailed in the section Phytoplankton and Zooplankton Analysis below). Five, 500 μl aliquots subsampled from a 10ml total extract volume were weighed after drying in a 60°C oven. The lipids of 16PH1 were measured at ALS (Kelso WA), but not measured at MIT.

Phytoplankton 2017

On May 17, 2017, 40 ml of pure lake water and three 1-L phytoplankton samples were collected just below the water surface at sites 1 and 8. Each sample was the result of three boat tows, each collected at 1 mph for 2 min (concentration factor ~134). Qualitative observations were made of 17PH84 with a light microscope (Zeiss Axiostar Plus Microscope 4907001303). All samples were normalized for TS (Figure S1). See the 2016 methods for the protocols used.

Particulate matter (PM) was measured as the phytoplankton sample solids that were retained on a glass fiber filter (Whatman, 25 mm diameter, glass fiber filter). A volumetric pipette was used to transfer 5 ml of phytoplankton sample from the middle of a shaken jar onto a single GFF (~1μm pore size). This was repeated three times each for samples.

The carbon and nitrogen contents of the PM at each site were measured with a CHN analyzer (Elementar Vario EL III, Mt. Laurel, NJ). 1-2 mg of dry material was removed from a sample after GFF filtration and placed into a 30 mg silver capsule (Consumers for Elemental Microanalysis; Pennsauken, NJ) and combusted at 950°C before carbon was measured as CO_2 and nitrogen as N_2 (hydrogen was not measured). 1-5 mg acetanilide standards (Merck KGaA, Damstadt Germany CAS 103-84-4, n=7) were used to calibrate the instrument (71 ± 2 %C and

10.1 ± 0.4 %N). The background signal from 30 mg blank silver capsules was 0.0080± 0.0007%C and 0.086 ± 0.005 %N (n=5).

PM samples were ashed (loss on ignition) to estimate the amount of inorganic material in each sample and reweighed for carbon and nitrogen content (Figure S1). Two PM samples from each site were baked at 450°C for 12 hours. The measured carbon and nitrogen contents of the ash were within the range of the background signal, and thus deemed negligible. Therefore, in this document, the measured carbon and nitrogen contents of the phytoplankton PM are referred to as the particulate organic carbon (POC) and particulate organic nitrogen (PON).

The chlorophyll in the phytoplankton samples was measured to estimate the POC:Chl-a ratio, a metric employed to confirm the presence of phytoplankton biomass. On the evening of field collection, the chlorophyll was extracted from the phytoplankton samples via Standard Methods [21]. 5 ml of a magnesium carbonate-saturated acetone solution were mixed with 7 ml of each phytoplankton sample. Samples were left in 4°C fridge for 80 min, then centrifuged at 1600 RPM for 20 min (Beckman Coulter Model GS-6 Swinging Bucket Centrifuge). The supernatant was poured off and the absorbances measured at 630, 647, 664 and 750 nm 5 times each in a quartz cuvette (l =1 cm) (Beckman Coulter UV/VIS Spectrophotometer, Model DU 800). In order to account for the pheophytin pigment, samples were acidified and remeasured at 665 nm.

The chlorophyll in the lake water was measured as an additional estimate on the tow concentration factor. Dilutions of the absorbance spectroscopy-determined chlorophyll concentrations (0.06 – 0.50 μg chlorophyll a/L) were used to standardize the fluorometer (Perkin-Elmer LS 50B 250). Fluorometer parameters were: 430nm excitation wavelength, 663nm emission wavelength, and beam slit width 10nm. The concentration in the lake water was measured 3 times per site against a chlorophyll-free water blank.

Zooplankton 2017

Zooplankton were collected on July 26, 2017, via repeated vertical pulls in the water from just off the bottom in 6-10 ft of water (Figure S2). The surface water temperature was 24.8°C. For each 2-liter zooplankton sample collected, the net was pulled 40-60 times by hand a vertical distance of ~3ft for a concentration factor of 20. Two, 2-L samples were collected from sites 1 and 8 (Figure S3). Each freshly collected zooplankton sample was depurated in the same lake water in which it was collected for 24 h and then filtered on a 120 μm Nitex screen to remove excreted phytoplankton (Figure S3). Samples were stored in a 10 ml vial at -80°C vial until extraction. The TS in the 120 μm Nitex screen filtered samples were weighed from 3-5 mg dry aliquots normalize zooplankton PCB concentrations on a dry mass basis (n=3). The carbon and nitrogen contents of the total solids were measured with the CHN (see 2017 phytoplankton method).

Phytoplankton and zooplankton extraction

Within three days of returning from the field, PCBs and lipids in the phytoplankton were measured by liquid-liquid extracting a 500-700 ml of each sample (Table 1). In order to estimate the reproducibility of the DCM lipid extraction method, sample 17PHS8.4 was extracted in triplicate (200 ml x 3). All volumes were extracted three times in a separatory funnel using a 10:1 water-to-DCM ratio and 1 min of vigorous shaking. After agitation, the entire volume was put into the freezer overnight to break the visible emulsion. The three DCM extracts were combined into a 200 ml round bottom flask (Figure S4). A few tablespoons of anhydrous sodium sulfate were added to each extract to remove any residual water.

The PCB and lipid contents in the zooplankton were extracted in a 40 ml vial three times. The sample vials were spiked with a known amount of surrogate standard (1.5-4.5 ng of each PCB congener via a composite solution in hexane), filled with DCM, capped and incubated on an orbital shaker at room temperature. After 1 day, the DCM was drained off from the separatory funnel and stored in a glass-stoppered round bottom flask.

Phytoplankton and zooplankton DCM extracts were concentrated using a multi-port condenser/concentration system (Starfish Multi-Experiment Work Station, Radleys Discovery Technologies, UK). The inner glass surface of the starfish apparatus was rinsed with 30 ml of DCM. The sample was attached by a ground glass fitting and concentrated for 1-2 hours at 40°C under 10-13 mmHg vacuum to ~1 ml volume.

In order to measure lipid contents, the 2017 phytoplankton and zooplankton extracts were pipetted into 5 ml volumetric flasks and brought up to volume. Lipid content was determined from a 300 µL subsample, placed on a tared Al pan, gently drying, and weighing using a microbalance. The remaining DCM solvent in the extract was concentrated to ~1 ml.

A silica column cleanup was used to remove excess organic matter that would interfere with GCMS analysis. All of the extracts were solvent exchanged to hexane under a gentle steam of nitrogen at room temperature. A 30 x 1 cm glass column was prepared with a small glass wool plug, 7 g of 5% deactivated $SiO2$ (100-200 mesh) and a ~2.5 cm anhydrous sodium sulfate cap. The sodium sulfate acts as a buffer region where the solvent can run dry without cracking the whole silica column. The column was rinsed with 20 ml DCM and then 20 ml hexane. The 1 ml hexane extracts were pipetted onto a silica column and three fractions eluted. Any precipitates in the concentrated extract were left in the bottom of the vial. The first fraction was eluted with 20 ml of hexane. The second fraction was eluted with 8-12 ml of 25% DCM and 75% hexane, until just before a yellow color band reached the column tip. Finally, a 20 ml 100 % DCM rinse was eluted and stored frozen. Fractions 1 and 2 were combined, nitrogen concentrated at room temperature and quantitatively transferred to an autosampler small volume glass insert with a final volume of ~25 µl.

Table 1. Phytoplankton and Zooplankton Sample Composition Summary

	2016 Phytoplankton MIT-AC				2017 Phytoplankton		2017 Zooplankton	
	16PHS1	16PHS2	16PHS5A	16PHS8	17PHS1.2	17PHS8.4	17ZOS1.D	17ZO8.E
f_{lipid} (dry TS basis, DCM)	0.013*			0.024	0.015	0.033	0.048	0.081
$f_{protein}$ (dry TS basis)					0.11	0.14	0.47	0.56
Tow net mesh (um)	63	63	63	63	63	63	150	150
Total solids (dry mg/L water)	590 ± 10	690 ± 20	700 ± 10	760 ± 10		1900 ± 100	172	85
DOC (mg tow filtrate/L water)	22.7 ± 0.5	77.5 ± 0.5	18.4 ± 0.3					
POC (mg filtered tow C/L water)					252	332	50 ± 2	45 ± 4
PON (mg filtered tow N/L water)					31	29	11.6 ± 0.4	9.8 ± 0.9
mol C: mol N					6.0	5.2	5.40 ± 0.06	5.03 ± 0.03
Volume extracted (L)	0.670	0.627	0.520		0.595	0.600		
Mass extracted (mg)	390		430	0400	1030	1140	298	129

Measured by ALS Environmental (Kelso, WA)

Phytoplankton lipid analysis

Using a DCM method, the lipid and target contaminants could be extracted in one step [47]. Lipid measurements vary with solvent used for extraction and organism tissue composition. Therefore, to validate the DCM method, it was compared to the traditional Bligh and Dyer [8] and a 50% DCM:50% hexane method, previously seen to be effective in *Nereis virens* worms [43].

In 2016, phytoplankton samples were extracted using DCM and 50% DCM:50% hexane. 100 ml phytoplankton sample was extracted three times with 10 ml of solvent. The extracts were combined, dried with anhydrous sodium sulfate and concentrated to 10 ml. Aliquots, 100 and 500 µl (5-8) were micropipetted into tared aluminum boats and dry weights determined gravimetrically (Cahn 25 Electrobalance, Cahn Inc. CA). The average mass extracted with the DCM:hexane solvent was 0.017 ± 0.003 mg lipid/100 µl. The average mass extracted with the 100% DCM solvent was 0.018 ± 0.001 mg lipid/100 µl. Given the TS concentrations in each suspension, the fraction lipid in DCM:hexane solvent was 0.037. Likewise, the fraction lipid in the DCM solvent was 0.041. These were calculated by multiplying the mass of lipid in the aliquot (n=5-9) by the volume of the solvent extract and divided by the total mass extracted (POM).

In 2017, the precision of the DCM method was assessed by extracting three 200 ml subsamples from 17PH84 (see below for method). These extracts were later recombined for GCMS analysis. The average weight of nine aliquots from a 5 ml volumetric flask was 0.26 ± 0.07 mg lipid/100 µl DCM (RSD=13%). The fraction lipid in the sample was 0.043.

This was compared to a Bligh and Dyer extraction on a previously frozen sample, 17PH83. The entire 630 ml sample was filtered using 12 GFFs under vacuum and then dried. 206.6 mg of dry phytoplankton were rehydrated to 80% water content (826.4 mg water) and then vortexed for 2 min with 1:2 methanol:chloroform (v/v, relative to wet sample mass). The filtrate was transferred to a graduated cylinder and separation/clarification allowed. The top methanol layer was aspirated away and the bottom chloroform/water lipid layer (~2.1 ml) removed and filtered through a small GFF. 2ml of the remaining phytoplankton biomass was washed with ~3ml of chloroform and filtered. The filtrate was blown down with helium gas at room temperature and transferred to a 5ml vial. 100 µl extracts were removed with a glass capillary pipette, dried and weighed. This was done three times resulting in an average of 0.23 ± 0.02 mg lipid/100 µl extract.

Freezing bursts the cell membrane and likely releases many components, both colloidal and dissolved. 1.07 gdw/L was recovered by the GFF of the thawed 17PH83, which is ~83% less than the 1.29 ± 0.05 g/L PM measured before freezing. Therefore, the total mass extracted was increased by 17% to account for the solids lost in the freeze thaw process. If freezing broke open cells, it was assumed that the freeze-leaked matter did not include significant lipid. Thus, the

13

calculated Bligh and Dyer lipid fraction was 0.047. The fraction of lipid measured using the Bligh and Dyer method were within the experimental uncertainty of the DCM extraction.

The fraction lipid for site 8 phytoplankton from both 2016 and 2017 as measured by different extraction methodologies (DCM, DCM:hexane, and Bligh and Dyer) was 0.042 ± 0.004. Therefore, we have a high degree of confidence in the DCM extraction method. Except for the 16PHS1, all other samples were measured for lipids simultaneous to the PCB extractions with only the DCM method. We use the relative deviation of the triplicate DCM extraction analysis to determine that the precision for the DCM method was 13%. Membrane lipid was not distinguished from storage lipid, as partition coefficients of these values vary by less than one order of magnitude (Table S6).

Protein analysis
The particulate organic nitrogen (PON) was measured to estimate the fraction of protein in each sample. Chlorophyll, nucleic acids, and cytoplasmic pools of inorganic nitrogen and free amino acids can represent a substantial pool of intracellular N [30]. A ratio of 4.78 g protein/g N was used instead of the standard convention (6.25 g protein/g N) to account for all of the non-protein nitrogen associated with the sample [31].

Field deployment of PE to measure the PCB concentrations in the water
A two-piece PE sampler was constructed and deployed to measure the PCB concentrations in the water and assess their vertical distribution. Aluminum frame samplers were inserted (via a 10 ft detachable pole) with the goal that ½ to ¾ of the PE would be in the sediment to capture the *in situ* pore water concentrations near the sediment surface, and the remaining PE would sample the overlying water concentrations. A grommeted mesh bag was floated above the metal frame with a ~1 m rope and buoy to sample the water column concentrations significantly above the bed (Figure S5).

The Booij et al. protocol was followed to clean and PRC-impregnate the PE before it was loaded into the sampler frames [10]. PE strips were cut from plastic sheets to the dimensions specified in Table S1 for both samplers. The PE was cleaned by soaking sequentially in a 2-L jar with DCM and then methanol, each for 24 h. Seven PRCs were loaded into the PE via a 80:20 (v/v) methanol:water solution and incubated on an orbital shaker table at room temperature for a week to equilibrate. The strips were then soaked twice for 24 h in deionized water to remove the methanol. The aluminum frame sampler was loaded with PRC-loaded PE the night before deployment, wrapped in foil and stored on ice. Part of the excess length from each of PE samplers were cut and reserved for t=0 PRC concentration analyses as well as some of the water column PE strips.

To assess the horizontal distribution of the PCB water concentrations each year, 10 samplers were placed along the edges of South Pond and Pegan Cove in Lake Cochituate (Table S1). In 2017, the average water depth was 6 ft, except for at site 7 where the depth was ~3ft. The

samplers at sites 3 and 5 were tied to a large buoy that floated just under the surface to protect them from vandalism.

Most of the samplers were located and recovered after about two months. To minimize PCB losses to the air, recovered samplers were wrapped in aluminum foil and stored in a cooler with ice packs. Of those deployed in 2016, the sampler at site 4A was not recovered, and the sampler at site 5A was found sitting flat on the bottom. PE frames were found to have over-penetrated at Sites 2A and 9 so they only captured concentrations in the surface sediment. Of those deployed in 2017, the sampler at site 7 was lost and the sampler at site 5A over-penetrated. Lost samplers were attributed to snagging and accidental removal by fishing lines, disturbed by recreational water skiers and/or power boats or vandalism.

PE extraction
On the day following field retrievals, PE samplers were unwrapped and visually inspected. There was no visual change to the sediment side of the sampler (PE remained clear) (Figure S6). Brown algae stained the water side, and this was wiped away with a Kimwipe® (Kimberly Clark Worldwide Inc.). The boundary between the two was marked by a thick black line that could not be wiped away with a clean, dry Kimwipe. This likely represents the depth where subsurface sediment minerals interact with oxygenated water. Depending on the site, there may also be a layer representing constantly resuspended sediments (so called 'fluff' layer). As dissolved metals in the anoxic sediment move to the interface they likely react with oxygen and oxidize, precipitating solids on the PE. The oxide coatings could have substantially affected the mass of the PE, and thus the length scale and time of diffusion for the PCBs.

The samplers were sectioned for discrete analysis at MIT and also so that a portion of samples could be sent to ALS Environmental for external analyses (Kelso WA). The water column samplers were divided in half (each slice ~7.5 x 10 cm). The sediment sampler PEs were split into 5 or 10 cm slices according to their distance from the sediment/bottom water interface and then they were divided in half. Some samplers did not go into the sediment evenly (i.e., Site 1). In these cases, the mass of PE analyzed at ALS and MIT was usually somewhat different.

The PCB concentrations in the PE slices were measured using DCM extraction. PE slices were blotted dry with a Kimwipe and each put into 40 ml amber vials. Vials were spiked with a known amount of surrogate standard (2.5-5.0 ng of each PCB congener via a composite solution), filled with DCM, capped, and incubated on an orbital shaker at room temperature. After at least 1 day, the DCM was poured off and stored in a glass-stoppered round bottom flask. The extraction was performed three times, and these extracts were combined.

All DCM extracts were concentrated using a multi-port condenser/concentration system (Starfish Multi-experiment Work Station, Radleys Discovery Technologies, Essex, UK) under 13 mmHg vacuum. ~1 ml concentrated extracts were pipetted quantitatively into 4 ml vials. The DCM

solvent in the extract was exchanged to hexane using a gentle stream of nitrogen at room temperature. The extracts were concentrated to 20-150 μL and transferred into 300 μL GCMS vial inserts. Each dried PE slice was weighed after extraction.

GCMS analysis of all field extracts

Immediately prior to the GC-MS analysis, 2.5 ng of each injection compound via a composite stock solution (25 μl of a 100 ng/ml stock solution) was added to each extract to determine final extract volumes. Standard compounds were run before, between every five, and after all field extracts. In addition to the PRC, surrogate, and injection compounds, the EPA-20 PCB mixture was analyzed to identify the target compounds and establish their response factors. Hexane blanks were run before and after standards.

PCBs were separated on a DB-5 MS 60m column (0.25 μm film thickness, 60 m x 0.25 mm ID, Agilent, Santa Clara, CA). The inlet temperature was at 300°C. Splitless, 1 μl injections were made under pulsed pressure (30psi) for 1 min. The helium carrier gas had a constant flow rate of 2 ml/ min. The gas chromatograph oven was programmed to ramp from 67°C to 188 at 25°/min, from 188-276° C at 1.5° C/min and finally from 276-300° C at 25° C/min, followed by a 3.6 min hold time. The total GC run time was 68 minutes. This program reflects a balance between peak separation and total analysis time.

All of the PCBs were detected using a JEOL GCmate MS. The instrument was operated in Selected Ion Mode (SIM) mode. The mass axis was calibrated between each sample using an internal standard (perfluorokerosene, PFK). TSS 2000 software was used to integrate the peak area of the most abundant m/z ion (quantitation) of each PCB (Shrader Analytical and Consulting Laboratories, Inc.). Baselines were corrected for automatically. The quantification and confirmation ions were used to verify each peak.

The retention times and response factors of target and standard compounds are listed in Table S2. Response factors are listed according to the groupings in which samples were analyzed. The response factor for PCBs varies based on a number of factors: the cleanliness of the injection port, the position of the column in the injection port, the condition of the capillary column, and the cleanliness of the source. These account for some of the variability in the factors seen between the 2016 and 2017 analyses.

Within a single analysis, response factors decrease with increasing congener hydrophobicity, possibly due to decreasing congener transfer onto the capillary column from the split/splitless injector. As the peak areas decrease, the compounds are more difficult to detect above instrument background signals. Congener peaks of approximately 2000 area units/μl are considered above background (minimum detection limit, MDL) with resulting concentrations of approximately 0.2-0.8 ng/g environmental sample (PE or plankton). Given 1 uL injections from

about 50 uL extracts, our reporting limits were ~0.6-1.8 ng/g, but varied with congener separation and dispersion.

On the GCMS we have measurement precision less than or equal to the RSDs of the standard curve determined RFs. The average calibration RSD for all of the analysis runs was 13 ± 4% (range = 8-23%). The accuracy of the RF in a given run depends on the condition of the manufacturer stock solution and the dilution from stock to a working standard solution. The EPA 20 stock solution (RPC-EPA-2, 100 μg/mL, acetone) was obtained from Ultra Scientific (N. Kingstown, RI), an industry certified and accredited laboratory. A single dilution was made from the manufacturer stock, to obtain a 1μg/ml hexane solution which was stored in a low-loss Certan® vial (Supelco™, Chromatography Division of Sigma Aldrich) to the 100ng/ml standard.

All extract volumes were calculated using volume recovery corrections on a congener-chlorine number basis to negate the effects of imprecise RF_{is}. The average volume (V_{is}) calculated from each injection standard was within 13% RSD (range) for all samples, which is about our instrument calibration precision.

$$Injection\ volume\ (ul) = V_{is} = \frac{spiking\ mass_{is}\ RF_{is}}{area_{is}}$$

All extracts analyzed by MIT-AC were spiked and calibrated with the same stock solution, so this method negated any imprecisions between the surrogate RFs. Larger volatilization losses during evaporation were expected for the lower molecular weight congeners. 3-Cl congeners were most sensitive to handling losses (15-50% recoveries). The average recoveries across a single congener typically reflected differences in sample handling. The uncertainty associated with making a GCMS target compound analysis was about 20%. This stemmed from the following sources: surrogate standard spiking mass ($mass_{ss}$,(25± 2 μl ~8%), area surrogate standard ($area_{ss}$), the area injection standard ($area_{is}$), the area target compound ($area_T$, ~5% each), response factor surrogate standard ($RF_{ss,}$ 13%,) and response factor EPA 20 compound (RF_{EPA}, 13%).

$$\%Surrogate\ Recovery = \%SS = \frac{area_{ss}V_{is}}{RF_{ss}\ spiking\ mass_{ss}}$$

$$C_{extract} = \frac{area_t V_{is}}{RF_{EPA}\ \%SS} = \frac{area_t\ mass_{ss}\ RF_{ss}}{RF_{EPA}\ area_{ss}\ area_{is}}$$

For the 2016 PE, the samples were not spiked and calibrated with the same surrogate stock solution. The injection and surrogate standards were assembled from high concentration manufacturer stocks of individual congeners stored in nonane. They have been used by multiple researchers over a period of a few years and there is uncertainty regarding losses to volatility, partitioning, and contamination. This, combined with the accuracy of multiple congener dilutions to the 1μg/ml stock solution, led to greater uncertainty in the extract volume and recovery calculations. The calibration surrogate standard was considered imprecise and inaccurate relative to the EPA 20 standard. The corresponding unlabeled $RF_{EPA\ 20}$ was used in place of the RF_{ss}.

PRC mass transfer model to determine CPE at equilibrium

A mass transfer model was used to correct for nonequilibrium of PCBs between the PE sampler and water phase (governed by 1st order kinetics) [10, 12, 42]. Specifically, the losses of PRCs from samplers to the environment were examined to determine the optimal correction for nonequilibrium conditions between target congeners in the PE and water. Targets are not initially present in the PE and PRCs are not present in the environment, therefore targets exclusively diffuse into the PE and PRCs exclusively diffuse out.

The PRC fractions remaining in the PE after their field deployments (f_{pe}) were calculated by comparing the t=0 PRC concentrations determined from subsamples of the field-deployed PE to the PRC remaining in the PE after field deployment. In the model, it is assumed that the PRCs instantaneously disperse into the surrounding environment. When all of the PRCs have left the PE, the corresponding sized target compounds have reached equilibrium.

When the PE is less than 100 μm thick and compounds have a log Kow > 5, it is assumed that the water boundary layer controls the rate of mass transfer [9, 11, 12, 42]. The fraction of PRC in the PE can be modeled with the exponential $f_{pe} = \frac{C}{C_{t=0}} = e^{-k_e t}$, where C_{pe} is the concentration measured in the PE [10]. In a well-mixed field site (thus infinite volume water conditions) the exchange rate coefficient, $k_e \left(\frac{1}{s}\right)$ is equal to $\frac{R_s}{K_{pew} m_{pe}}$. Under water boundary layer control, the sampling rate is $R_s(\frac{cm^3}{s}) = k_0 A$ and the overall mass-transfer coefficient equals the mass transfer coefficient for the water phase. $k_0 = k_w = \frac{D_w}{\delta}$ [11, 42]. Therefore $k_e = \frac{D_w}{K_{pew} L_{pe} \delta}$, where D_w is the diffusivity of the PCBs. D_w, K_{pe} and L_{pe} are measurable quantities that have been studied and reported in the literature.

The boundary layer thickness depends on the turbulence of the environment and the diffusivity of the PCB in water. The f_{pe}, were fit with a least squares regression model to estimate a single average (this assumes solute independent boundary layer thickness even though it is $\sim MW^{-0.24}$). The quality of the fit was described by the root mean squared error (RMSE). The intricacies of the fit were evaluated by comparing the measured and $\boldsymbol{\delta}$-calculated fractional approaches to equilibrium, feqs.

The fractional accumulations of the target compounds were back calculated with the PRC fitted $\boldsymbol{\delta}$. The measured target concentrations in the polyethylene were then equilibrium corrected: $C_{pe, eq} = 1/(1-f_{pe}) = 1/f_{eq}$. The uncertainty on the $C_{pe,eq}$ at each site was evaluated from two components of the PRC with the closest K_{ow}: the RSD of the t=0 PRC concentrations and the RSD of the PRC measured vs fitted f_{pe} values. The K_{pew} was used to calculate the freely dissolved water concentrations from the C_{PE} at equilibrium: $C_w = C_{pe,eq}/K_{pew}$.

Equilibrium Estimates of Phytoplankton Concentrations (Cpl*) from Water Concentrations

In order to evaluate the equilibrium status of the phytoplankton and zooplankton samples with the dissolved water concentration, a sorption estimate was made based on the phytoplankton f_{lipid} and K_{lw}. The reported uncertainty of the estimated phytoplankton concentrations reflected the uncertainty associated with the average water concentrations in Pegan Cove for site 1 and South Pond for site 8 and the fraction lipid (13%). When it was necessary to determine significant differences, literature reported uncertainties of the partition coefficients were considered.

Selection of partition (K) and diffusion (D) coefficients from the literature

In the absence of experimental parameters, Abraham coefficient based ppLFERS (poly parameter linear free energy relationships) and K_{ow} based LFERS (linear free energy relationships) were used to estimate partition constants. The van Noort updated PCB coefficients were used in place of the Abraham coefficients where possible. The lipid water partition coefficients (K_{lw}) were calculated with the Endo et al. ppLFER [17]. log K_{lw} values at 25°C vary between 5.26 ± 0.21 and 8.79 ± 0.28 L water /kg lipid. The K_{pw} partition coefficients were calculated with the fish protein ppLFER reported by Geisler et al. [19]. The magnitude of these were 70 to 250 times smaller than their $K_{lipid\,water}$ counterparts. The values of all partition coefficients are reported in tables S3 and S4.

Experimentally determined K_{pew} from Choi et al. were employed [15]. Otherwise the K_{pew} was calculated from the Choi LFER and based on Hawker and O'Connell K_{ow}s [24] to estimate the Kpe. The uncertainty associated with the measured values averaged 0.03 log units (range 0.01-0.28 log units). The average RSD (28%) of PCBs reported in the literature was used for the K_{ow} predicted K_{pew}[29]. log K_{pew} values at 20°C vary between log 4.60 and log 7.89.

Several studies have considered the effects on partition coefficients of water and organic phases like PE [1, 11] and lipid [17, 19] in an effort to estimate phase specific excess enthalpies over environmentally relevant temperatures. The data are limited and do not consider the whole range of PCBs measured in this study. It was assumed that the changes in partitioning for all phases could be estimated with a ΔH_{ow} ppLFER [37]. The ΔH_{ow} for the range of PCBs studied from smallest to largest congeners ranged between -16 and -35 kJ/mol, which indicates that from 12 to 25°C, Ks decrease by a factor of 25-50%.

The diffusivity in water, D_w, was calculated from the temperature dependent (via solvent viscosity) formula of Hayduk and Laudie [25]. Comparison of these values with the Schwarzenbach et al. relationship based on the data of Yaws [49] indicated that the D_w of PCBs can vary by 0.01-0.16 log units, depending on the source of the model: 0.11 log unit variation

Hayduk and Laudie vs Yaws relationship and 0.16 log units with 12°C change. All the values are listed in Table S5.

Results

Phytoplankton and Zooplankton Sample Composition

2016 Phytoplankton

In initial assessments of phytoplankton tow samples, there was some concern that organic matter buildup over the tow duration could decrease the net efficiency. This would adversely affect our measurement of PCB concentrations because we would be underestimating phytoplankton mass due to colloid collection. The average TS of the phytoplankton samples at Sites 1 and 8 was 670 ± 90 mg/L (Table 1). The DOC accounted for ~6% of the TS, a minor fraction of the extracted mass.

2017 Phytoplankton

A sample of Lake Cochituate phytoplankton diatoms is shown in Figure 2. The composition of the Site 8 tow concentrated 2017 phytoplankton lake samples were examined via microscopy. These observations indicate that of a natural population of freshwater diatoms. The phytoplankton samples appeared greenish brown in color. A few diatom species, *Synedra, Tabellaria, Stephanodiscus* and *Asterionella,* dominated the microscopy fields. These same species were observed by George Whipple in 1896 [48]. Some detritus and an isolated zooplankton were observed among the diatoms (Figure S7). No microscope observations of Site 1 phytoplankton samples were made.

TS, POC, PON and chlorophyll measurements between the two sites were similar. In 17PHS8.4 phytoplankton, the measured PM accounts for 78% of the total solids in the sample. PM was relatively uniform across six samples from the two sites, with an average PM of 1.4 ± 0.2 g/L. The PM at 17PH1 and 17PH8 were not significantly different (1.4 ± 0.2 g/L at site 1 and 1.5 ± 0.2 at site 8).

The POC:PON ratios together with the ash content of the PM suggest that the sample solids comprised of diatoms (Table 1). The average C:N molar ratio of the six phytoplankton samples from two sites was 6.3 ± 0.8, consistent with Redfield stoichiometry (6.6) of nutrient replete phytoplankton populations (Table 2). The differences between sites were not significant but there was some variability among samples from a single site. The average POC and PON at 17PHS1 was 20 ± 1% and 2.5% ± 0.3% of the PM, and the average at 17PHS8 was 23 ± 1% and 2.9 ± 0.1 (Table 1). The ash content determined at 450°C of the PM samples was not significantly different at sites 1 and 8 and the average was 48 ± 5%. (50 ± 7% at site 1 and 46 ± 6% at site 8). This was inferred to be silica based on microscope observations of freshwater diatoms.

Figure 2. (left) Lake Cochituate phytoplankton diatoms (17PHS8.4) (right) Lake Cochituate copepod (17ZOS8)
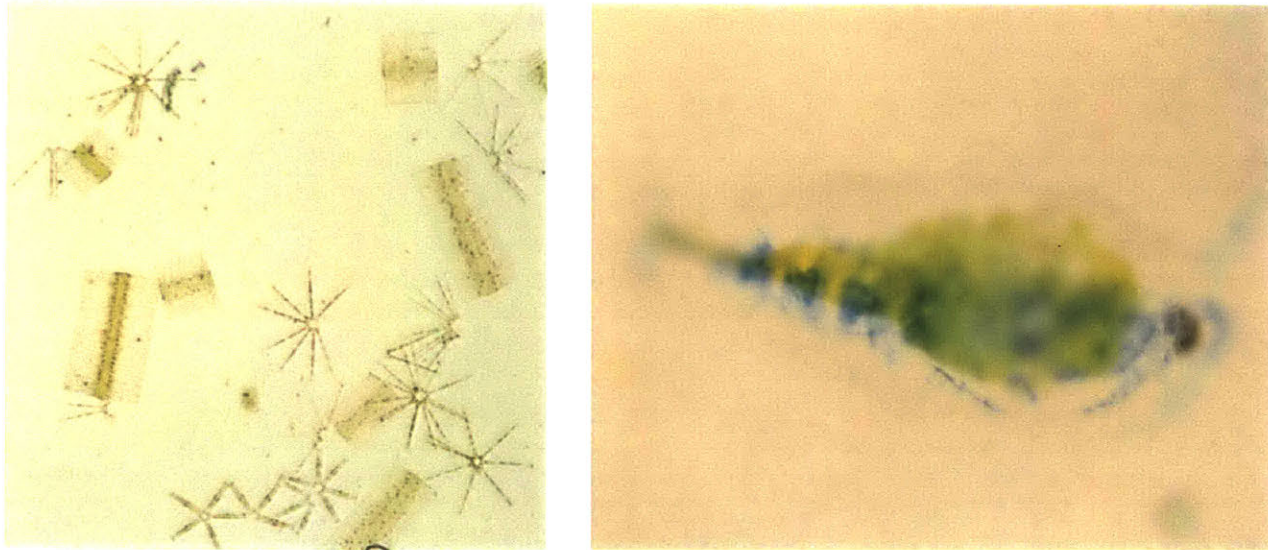
When compared with the POC, chlorophyll measurements further support the presence of phytoplankton populations (Table 2). Chlorophyll was extracted from whole water samples, and reflect the chlorophyll associated with the TS. Some variability was observed within samples from a single site. The average concentrations were similar between sites 1 and 8. In site 1, the average chl-*a*, chl-*b* and chl-*c* concentrations (5 replicate analyses) were 2180 ± 50 µg/L, 390 ± 90 µg/L, and 1300 ± 80 µg/L. For site 8 the average concentrations were 2500 ± 30 µg/L, 200 ± 100 µg/L and 1300 ± 200 µg/L. The POC:chl-*a* for the six phytoplankton samples was 129 ± 24, which is within the wide range of laboratory and field study reported values ($6 - 333$) [26]. These chlorophyll numbers suggest a high percentage phytoplankton mass in the sample.

The chlorophyll concentration factors were 60 ± 20. The chl-*a* extracted from the TS in sites 1 and 8 unconcentrated lake water were 50 µg/L and 30 µg/L, respectively (Table 2). These values suggest that the parameter tow concentration factor severely overestimated biomass collection. The POC:chl-*a* ratio from the tow samples were applied to the lake water chl-*a* to estimate the *in situ* phytoplankton concentrations: 6 and 4.9 mg phytoplanktonPOC/L lake water (28 mg dry phytoplankton/L lake water) at sites 1 and 8, respectively. These estimates are useful for determining plankton inputs in food web models.

Table 2. Chlorophyll, POC:Chl-*a* and C:N ratios of 2017 phytoplankton samples

Sample	Chlorophyll (mg/L)			POC:Chl-a	C:N
	chl-a	chl-b	chl-c		
Lake Water Site 1	0.053				
17PHS1.1	2.13 ± 0.03	0.29 ± 0.01	1.21 ± 0.06	106	5.5
17PHS1.2	2.21 ± 0.06	0.39 ± 0.04	1.33 ± 0.08	112	6.0
17PHS1.3	2.18 ± 0.02	0.50 ± 0.01	1.35 ± 0.01	136	6.7
Lake Water Site 8	0.035				
17PHS8.1	2.64 ± 0.05	0.23 ± 0.02	1.41 ± 0.05	156	7.6
17PHS8.3	2.83 ± 0.03	0.40 ± 0.02	1.52 ± 0.06	105	6.7
17PHS8.4	2.09 ± 0.03	0.09 ± 0.03	0.84 ± 0.07	157	5.2
Average 17PHS1	2.18 ± 0.05	0.39 ± 0.09	1.30 ± 0.08	118 ± 16	6.1 ± 0.6
Average 17PHS8	2.5 ± 0.3	0.2 ± 0.1	1.3 ± 0.3	140 ± 30	6.5 ± 1.2
Average 17PH	2.4 ± 0.3	0.3 ± 0.1	1.3 ± 0.2	129 ± 24	6.3 ± 0.8

2017 Zooplankton

A subsample from 17ZOS8.E was diluted and examined microscopically. Copepod species were observed (Figure 2). The TS of 17ZOS1.D and 17ZOS8.E were 172 and 85 mg/L, respectively. C and N measurements at both sites were quite similar. According to the CHN analyses, the carbon zooplankton solids were 45 ± 4% (n=3) and 50 ± 2 at sites 1 and 8, respectively (Table 1). The nitrogen contents at these sites were 9.8% ± 0.9% and 10% ± 1%. The differences between samples at two sites were not significant. The average carbon content exactly reflects the precise value (48 ± 1%) reported for crustacean zooplanktons in a humic-rich lake over different seasons and nutrient cycles [2]. The average C:N molar ratio at the two sites were significantly different, 5.40 ± 0.06 and 5.03 ± 0.03. The site 1, the ratio was within the ratio of the lake zooplanktons (5.4-6.0) and the measured ratio for nitrogen replete coastal marine copepods (5.5-6) [46]. The site 8 was below these literature values, suggesting that the population distributions were unique at each site or that more nonliving organic matter was collected in the site 8 sample.

Lipid and Protein Contents of Phytoplankton 2016, Phytoplankton 2017 and Zooplankton 2017

Within a single site, the fraction lipid of zooplankton was about twice that of the phytoplankton (Table 1). The f_{lipid} of the samples at site 8 were twice the f_{lipid} of the samples at site 1. The f_{lipid} of 17PHS1.2 and 17PHS8.4 samples were 0.019 and 0.043, respectively (TS dry weight basis). The f_{lipid} of the 17ZOS1.D and 17ZOS8.E were 0.048 and 0.081 (TS dry weight basis). The differences in phytoplankton lipids observed between the two sites could reflect differences in the species distributions or conditions of environmental stress on the same populations.

In addition, we observed that the fraction lipid for site 8 phytoplankton measured in 2016 and 2017 were different by a factor of 2 (see lipid method above). The fraction lipids in 2016 were

not measured at site 1, but ALS environmental measured the lipids at 0.013. Similar fraction lipids (0.02) have been reported for field populations in food web model referenced studies [34, 39]. Similar fraction lipid of copepods in the ocean have been reported (0.02-0.10) [28, 50].

The differences observed between fraction lipid in site 1 and site 8 samples were not mirrored in the estimated protein (Table 1). There were, however, differences between the protein content in phytoplankton and zooplankton. The average fraction protein estimated from the nitrogen contents of 17PHS1 and 17PHS8 were 0.12 ± 0.02 and 0.135 ± 0.009 (TS dry weight basis), respectively. The average fraction protein estimated for 17ZOS1.D was 0.47 and for 17ZOS8.E was 0.55.

The protein fraction and the carbohydrate fractions in the phytoplankton and zooplankton contributed minimally to the total PCB bioburden. The carbohydrate sorptive capacity is 3-4 orders of magnitude smaller than the lipid capacity (Table S9), therefore the carbohydrate fraction of the samples was not considered. As evidenced by the K_{pw} partition coefficients (Table S6), the protein bioburden increases with increasing congener hydrophobicity. In this study, the zooplankton $f_{protein}$:f_{lipid} ratio was 10, and the protein contributed 13%-7% of the PCB accumulation. The phytoplankton $f_{protein}$:f_{lipid} ratio was 4-6 and protein contributed 6-2%. Based on these distributions, and since the protein was not measured in 2016, the protein fraction was considered unimportant and excluded from Cpl* calculations.

Freely Dissolved PCBs Measured in Lake Cochituate Water

This part of the study looks at PE samplers from the following locations: 16PE05 Pegan Cove (PC) 0-5 cm PE samplers sites 1, 2, 2A and 3 and South Pond (SP) samplers from sites 7 and 8; 16PEWC PC sites 1, 2, 2A and 3, and SP sites 7, 8, and 9; 17PE05 PC sites 1, 3 and 4, and SP sites 8 and 9; 17PEWC PC sites 1, 2 and 4, and SP site 8. Site 10, also located in SP, yielded results which did not fit the PCB pattern that emerged from the other SP PE samplers. Therefore, for the purposes of the following comparisons, it was excluded from the average "South Pond" concentrations.

The 2016 PE extracts, surrogate recoveries for 3-7 Cl were similar across congeners (average RSD of concentrations was within acceptable limits (Table S7). For the 4-7 Cl congeners, the surrogate recoveries for the 2017 PE analyzed were similar and within acceptable limits. Average recoveries of the 3-Cl surrogate for PE 0-5 and WC samplers, respectively, were 39% and 27%, which are somewhat low may reflect losses during nitrogen solvent evaporations. Fraction PE for PRCS 47 through 178 in 16PE05 at sites 7 and 10 were recovered with hundreds to thousands of percents. These suggest sample contamination, extract contamination, or wild t=0 disequilibria and the samples were excluded from further analysis (Table S9).

PRC Corrections to Equilibrium

Since it takes much longer than 57 days for the PE samplers to reach equilibrium, a diffusion model was used to convert the measured PRC values in the PE values into their equilibrium concentrations. The measured and fitted values are shown in Table S9. The measured fraction of PRCs (f_{pe}) in the PE and fitted f_{pe} values did not always agree within the analytical uncertainty. For example, within the 16WCPE, *at most*, the exponential model fit significantly overestimated fpe, PRC 54 by 0.24± 0.03 and *at least* underestimated f_{pe}.PRC 47, by 0.10 ± 0.03 in the 16WCPE samples. For 17WCPE, *at least* it underestimated f_{pe}, PRC 47 by 0.15 ± 0.05 and 0.07 overestimated f_{pe},PRC 178 by 0.1. The model PRC model affects measured values truly reflect the physical reality, the fitted values artificially decrease or increase the PE equilibrium correction factor, and thus the estimated C_{water} values. When PCBs mostly equilibrated the discrepancies between the model and fitted values are less important. quilibrium correction factors are near to 1 and thus, any over- or under-predictions have minor consequences.

Despite differences in the model, measured fractional recoveries of the PRCs in the PE were consistent between most of the samplers deployed in a given year. For example, the average fraction of PRC 101 in the 17PE05 and 17PEWC, respectively, were 0.3 ± 0.2 and 0.4 ± 0.1. Of the 2017 PE, only 17PE05 site 2 stands out with the lowest recoveries (ie, fpe,PRC 101 was 0.07). In the absence of analytical errors, increased mass transfer between the water and PE at site 2 could be due to relatively higher turbulence or laminar flows.

PRC recoveries of the intermediate congeners suggested that the field samplers were more equilibrated in 2017 than they were in 2016. The average measured fraction of PRC 101, in the PE in 2016 and 2017 were significantly different at 0.9 ± 0.3 and 0.4 ± 0.1, respectively. Higher temperatures, increased USGS gauge levels, in the spring as compared to the fall all present in favor of a more complete equilibration of field samplers in 2017. PRCs that could be distinguished as less than 100% recovered (4 in 2016 and 5 in 2017) were used to fit the exponential model. Therefore, the others were eliminated from the fit and PRCs were eliminated so that only those PRCs whose measured recoveries were certainly less than 100% were used to train the model.

Thinner boundary layer thicknesses in the 0-5 cm PE as compared to the WC PE suggested faster equilibration. The exponential fit yielded physically reasonable boundary layer thicknesses. Except at site 9 (BL thickness=760 um), the boundary layer thicknesses for 16PE05 and 16PEWC samplers were 350 ± 100 (230 - 490 um) and 410 ± 30 um. The average 17PEWC and 17PE05 boundary layer thicknesses were 200 ± 70 and 120 ± 40, respectively. While the selection of K_{pew} and D_w (ie +0.4 log units) changed the fitted boundary layer thicknesses by up to a few hundred microns, it only affected the f_{pe} fits ~1%. The boundary layer thicknesses estimated by these results were congruent with those previously measured in field samples. Boundary layer thicknesses need to reflect physical and environmentally relevant conditions, but in terms of predicting the accurate C_w concentrations, the fitted f_{pe} are of primary concern.

In 16PE05 and 16PEWC, the more hydrophobic PCBs were most sensitive to inaccurate fits. The least equilibrated congeners require the largest equilibrium correction factors. For example, the average measured 16PEWC fractions PE for PRCs 111, 138 and 178, respectively, were 102% ± 16%, 102% ± 16% (different feqs, same average) and 139% ± 32%. When measured fractional equilibrations were low (<5%), the corresponding correction factors (CFs) were 20 or more: $CF_{equilibrium} = \frac{C_{pe}^{eq}}{C_{pe,t}} = \frac{1}{1-f_{pe}}$. The average 16PEWC fit estimated CFs for PRCs 111, 138 and 178 were 10 ± 3, 18 ± 5 and 38 ± 11, respectively. These demonstrate how the estimated feq for the large PRC fits are more uncertain as the CFs increase. The average corresponding RSD from the PRC fits across congeners were 93% , 77% and 108%. Based on these analyses, it is important to remember in future discussions that the 2016 model increasingly lacks predictive power for target congeners as hydrophobicity increases from PCB 111 through PCB 209.

The 2017 PE samplers were less sensitive to fit overestimation than the 2016 PE samplers because they were equilibrated enough to require modest correction factors. Measured C_{pe},PRCs indicated that ~20% of the largest PRCs were lost to the environment. Even though PRC 178 was overestimated in the 2017 PE fits, the average measured correction factor was 4, and the fit correction factor was 6, or a 1.2 times larger. The average corresponding RSD with the PRC fit across congeners was 13% ± 10%. Therefore, the 17PE model discrepancies and equilibrium corrections had minor consequences on the uncertainty of C_w values.

There was no difference between the equilibrium concentrations measured in site 1 and the average concentrations measured in Pegan Cove. For example, the equilibrium water concentration for PCB 153 at 16PEWC.S1 was 26 pg/L and the average water concentration in Pegan cove was 26 ± 3 pg/L. Similarly, there was no difference between the average concentrations in South Pond and the concentrations measured at site 8. The concentration of PCB 153 at 16PEWCS8 was 9 pg/L and the average was 8 ± 2 pg/L. Therefore, in future analyses, the site 1 and site 8 water concentrations are reported as the average concentrations and their standard deviations (1 sigma) of all the samplers from Pegan Cove and South Pond, respectively.

Figure 3 summarizes the equilibrium water concentrations predicted from the PRC model at site 1 and site 8 from 2016 and 2017. The figure shows that there is not much difference between the 0-5 cm and water column measurements. In 2016 site 1, for PCBs 52, 101, 153 and 187 the concentrations in the 0-5cm and WC samplers, respectively, were 52 ± 21 and 38 ± 2, 30 ± 7 and 18 ± 2, 42 ± 15 and 26 ± 3, and 17 ± 7 and 10 ± 1 pg/L. In 2017 at site 1, the corresponding concentrations were 60 ± 36 and 51 ± 6, 10 ± 3 and 11 ± 2, 12 ± 6 and 15 ± 3, and 4 ± 2 and 5 ± 1 pg/L.

Figure 3 Equilibrium water concentrations
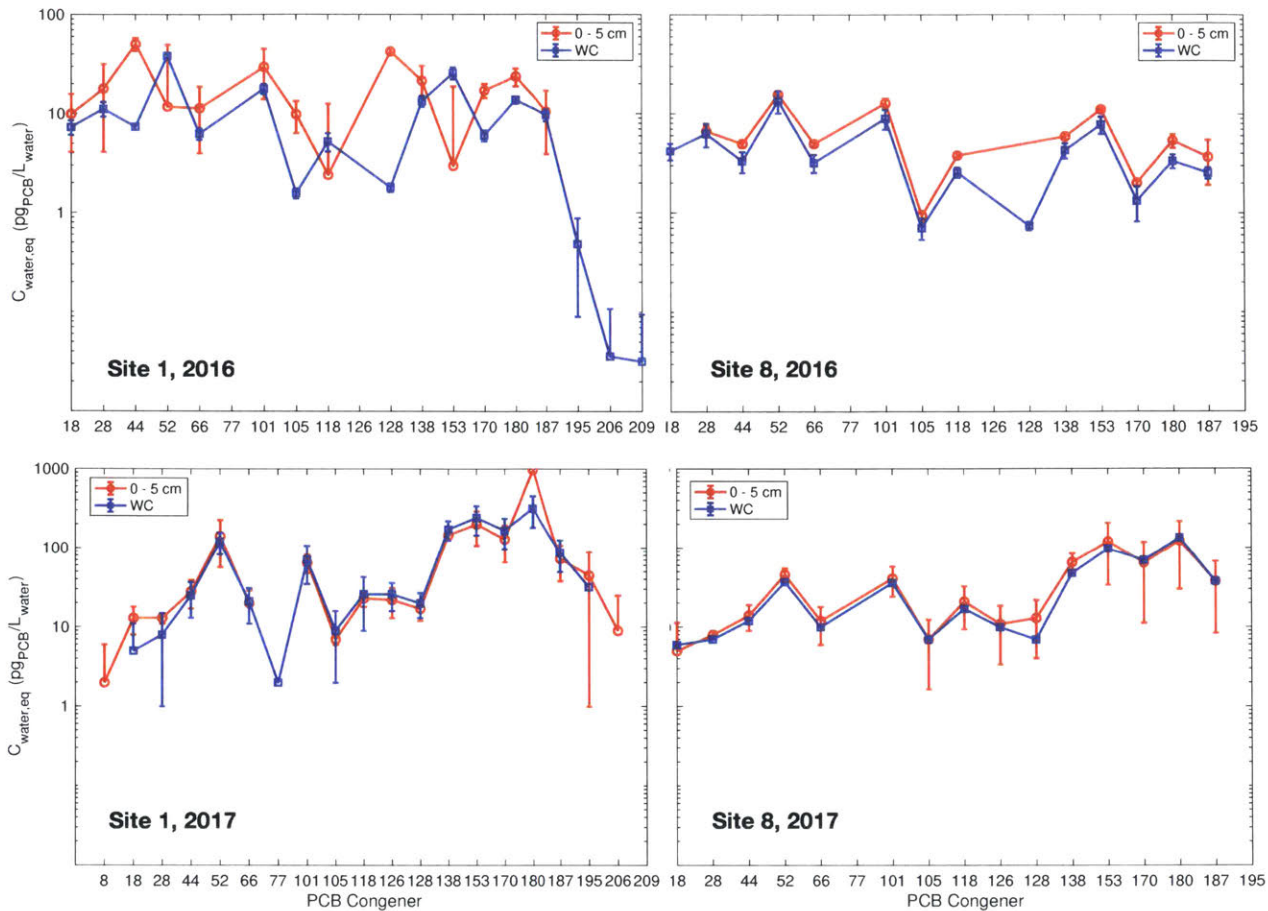
PCBs Measured in Phytoplankton and Zooplankton

In Figure 5, the concentrations of PCBs in measured and estimated from water column plankton from site 1 and site 8 in 2016 and 2017. The water column data was obtained by applying the lipid-water partition constant to the data in Fig. 4. For clarity, only the estimates for water column data are shown since they are similar to the 0-5 cm data.

For the purposes of this study, the concentrations of four abundant congeners measured in the phytoplankton are focused on: PCB 52 (4-Cl), PCB 101 (5-Cl), PCB 153 (6-Cl) and PCB 180 (7-Cl). Of these four congeners, two coelute with other PCBs. PCB 52 coelutes with congener PCB 43. PCB 43 is abundant in lower chlorinated Aroclor mixtures which are not expected to be seen in Lake Cochituate. PCB 153 is the congener of most abundant mass. Although it has a small shoulder coelution with PCB 132, it presents in 3:1 predominance over congener 132 in Aroclor mixtures 1254 or 1260.

For the extract concentrations, the calibration curve measures of specific congeners showed a relative error of maximum 20%; implying that the propagated errors on the inferred

phytoplankton concentrations would be 25% given uncertainties in TS values and volumes extracted. Measured extract volumes were small (16-122 µl), but they were calculated with 4-12% precision (Table S14). Measured concentrations were surrogate recovery corrected with their chlorine number equivalent congener. The average 4-7 Cl surrogate recoveries for the 2016 phytoplankton were between 75-118%, with corresponding RSD 14-7% (Table S14). The 2017 phytoplankton recoveries ranged 47-86% with corresponding RSD 6-10%. The zooplankton recoveries were 83-99% with corresponding RSD 10-15%. Average RSDs between 6-15% suggest that the extracts processed together were handled similarly, even when volumes were different.

The relationship between congeners from each 2016 phytoplankton, 2017 phytoplankton and 2017 zooplankton sample are consistent with that of a mixed Aroclor signature. In Aroclor 1260, the relative abundances of PCB 101, PCB 138 and PCB 187. PCB 52 are 5, 6 and 4%, respectively [36]. There is no contribution to PCB 52 in Aroclor 1260. PCB 52 is present in Aroclor 1242 and 1354 at 4 and 5%, respectively. Apell et al. reports a theoretical concentration of an Aroclor mixture contain 37% Aroclor 1254 and 63% Aroclor 1260 [3].

Figure 4 Concentration of PCBs in plankton and estimated from truly dissolved water column data obtained using passive samplers.

27
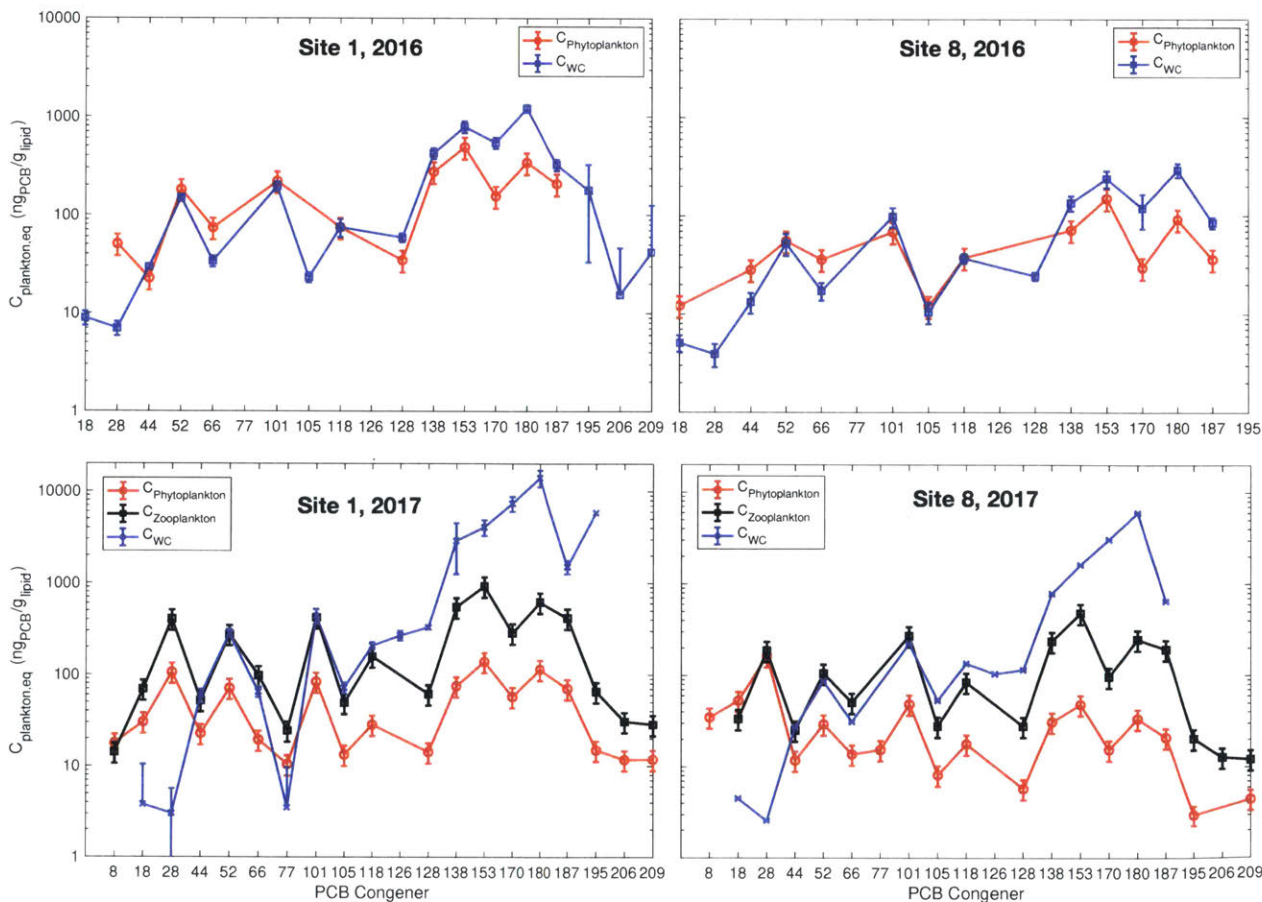
Figure 4 (top left) implies that the PCBs were in equilibrium between the phytoplankton and the water column in 2016. In PH16S1, concentrations for PCB 52, PCB 101, PCB 153 and PCB 187 measured at 180, 220, 500 and 210 ng/g lipid. The water column estimated phytoplankton concentrations at equilibrium were 150, 200, 800 and 330 ng/g lipid. The corresponding concentrations measured in 16PHS8 were 60, 70, 70 and 35 ng/g lipid and estimated via 16PEWCS8 at equilibrium were 50, 100, 240 and 90 ng/g. The water column-predicted and phytoplankton-measured concentrations for PCB 52 and PCB 101 agree within 20% at site 1 and 30% at site 8 of the measured value. At site 8, the predicted concentrations for PCB 153 and 187 overestimate the measured by a factor of 1.6, which is within the uncertainty of the mass transfer model for 2016.

Especially for larger congeners in the phytoplankton spring 2017, samplers appear undersaturated with respect to concentrations expected from water concentrations, and increasingly so with hydrophobicity (Figure 4, bottom). For example, in 17PHS1 the measured concentrations of PCB 52, PCB 101, PCB 153 and PCB 187 were 70, 84, 140 and 71 ng/g lipid. The predicted concentrations were 150, 200, 800 and 330 ng/g lipid. The predicted PCB 153 and PCB 187 were 6 and 5 times higher than the measured. The predicted PCB 52 and PCB 101 were only 2 times higher than the measured. In 17PHS8 the measured concentrations were 30, 50, 50 and 20 ng/g lipid and 17ZOS8 were 100, 270, 480 and 190 ng/g lipid. At site 8 predicted 50, 100, 240 and 90 ng/g lipid. The predicted PCB 52 and 101 were within a factor of 2 of the measured, but PCBs 153 and 187 were 5 and 4 times overestimated. That phytoplankton might be undersaturated in the spring is consistent with past studies in which rapidly growing plankton are found to be undersaturated ([41]). When we consider that errors asccociated with the PRC corrections (factor of 2), thatthe K_{pew} constants have uncertainty between log 0.02-0.28 (increasing with hydrophobicity), and the K_{lw} constants (are 0.21-0.28 log units), these differences seem less significantly clear. Therefore, considering all of the elements of uncertainty, it is likely that the smaller congeners (PCB 101 and smaller) are close to equilibrium.

Similar to analyses on the 2017 phytoplankton, the zooplankton were approximately equilibrated, relative to expectations from the predicted from the water. In 2017, the measured zooplankton concentrations were 4-10 times larger than the phytoplankton concentrations (Figure 4). At site 1, the zooplankton concentration for PCB 153 was 280 ng/g lipid or 5 times higher than the measured phytoplankton concentration. The most drastic differences by congener were seen in site 8 where, for example, PCB 187 was 10 times concentrated (200 ng/g lipid zoo versus 20 ng/g lipid phyto) while PCB 52 was only 4 times more concentrated (100 ng/g lipid zoo versus 30 g/g lipid phyto).

In 2017, the measured phytoplankton concentrations were 2±1 times more concentrated at site 1 than they were at site 8 (Figure 5, bottom). However, this observation was somewhat congener dependent. The measured phytoplankton concentrations were ~2 times higher in 2016 than they were in 2017 (Figure 5, top). For example, at site 1 PCB 153 was 180 and 70 pg PCB/L in fall 2016 and spring 2017, respectively. More broadly, the ratios of 2017:2016 concentrations were 3

± 1 and 2.0± 0.5, at sites 1 and 8, respectively. There was no obvious correlation of the difference with hydrophobicity. If the differences between the fraction lipid in 2016 (1.5 and 1.8x lower than 2017 at sites 1 and 8, respectively) are not real, they could explain these differences.

Figure 5. Concentrations in the water and phytoplankton in 2016 and 2017 at Sites 1 and 8.
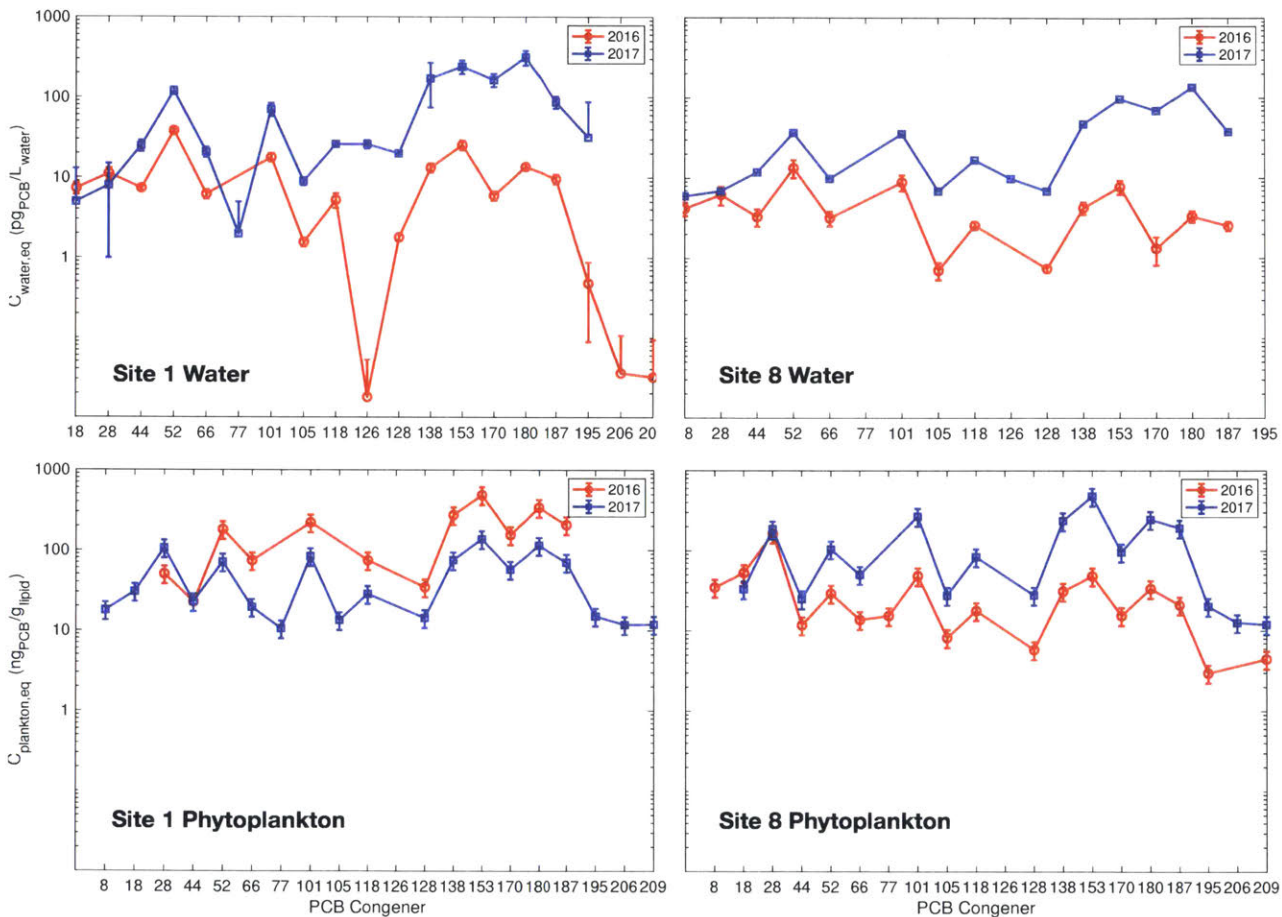
Conclusions

In this work, a passive sampling method were applied to measure the truly dissolved chemical concentrations of PCBs in Lake Cochituate water just above the sediment interface (0-5 cm) and in the water column. There were no significant differences observed between concentrations in samples from 0-5 cm and the WC (i.e., 1 m above the bed). Measurements of the PCB concentrations in phytoplankton and zooplankton were made at Lake Cochituate in Natick, MA, in Fall 2016 and Spring 2017. The phytoplankton and zooplankton samples were characterized by the fraction of lipid, protein, and organic carbon. The high chlorophyll to PC ratio along with the green color of the samples suggested that we measured PCBs in samples that comprised mostly phytoplankton. A phytoplankton sorption estimate was made from the freely dissolved

water concentrations, based on the lipid water partitioning coefficients, K_{lw}. In fall 2016, PCBs in the phytoplankton lipid were at equilibrium with the surrounding water. It spring 2017, it appeared that most of the concenters were equilibrated. It is possible that the large congeners of the zooplankton and phytoplankton were underequilibrated, but due to large uncertainties in equilibrium water concentration estimates and lipid partition coefficients this is not clear. It was observed that the lipid normalized zooplankton concentrations were significantly higher than the phytoplankton concentrations. If these are different, food web models should consider zooplankton with a balance of intakes and outtakes.

Analytical Recommendations

In the future, it is recommended that phytoplankton samples from a single site are mixed before they are analyzed to account for heterogeneity of samples collected from the same site. In 2016 there was some difficulties with PRC loadings, including uncertainty in the weights of the PE due to variability in PE thicknesses. It is recommended that PE is weighed before deployment to ensure uniform thickness and therefore uniform mass transfer rates of PRCs and target PCBs.

Bibliography

[1]   Adams, R.G. et al. 2007. Polyethylene Devices: Passive Samplers for Measuring Dissolved Hydrophobic Organic Compounds in Aquatic Environments. *Environmental Science & Technology*. 41, 4 (Feb. 2007), 1317–1323. DOI:https://doi.org/10.1021/es0621593.

[2]   Andersen, T. and Hessen, D.O. 1991. Carbon, nitrogen, and phosphorus content of freshwater zooplankton. *Limnology and Oceanography*. 36, 4 (Jun. 1991), 807–814. DOI:https://doi.org/10.4319/lo.1991.36.4.0807.

[3]   Apell, J.N. Using Polyethylene Passive Sampling to Assess Transport of Polychlorinated Biphenyls (PCBs) between Contaminated Sediments, Water, and Biota. 189.

[4]   Apell, J.N. and Gschwend, P.M. 2014. Validating the Use of Performance Reference Compounds in Passive Samplers to Assess Porewater Concentrations in Sediment Beds. *Environmental Science & Technology*. 48, 17 (Sep. 2014), 10301–10307. DOI:https://doi.org/10.1021/es502694g.

[5]   Arnot, J.A. and Gobas, F.A.P.C. 2004. A food web bioaccumulation model for organic chemicals in aquatic ecosystems. *Environmental Toxicology and Chemistry*. 23, 10 (2004), 2343–2355. DOI:https://doi.org/10.1897/03-438.

[6]   Axelman, J. et al. Field Measurements of PCB Partitioning between Water and Planktonic Organisms: Influence of Growth, Particle Size, and Solute–Solvent Interactions. 5.

[7]   Berglund, O. et al. 2001. The Effect of Lake Trophy on Lipid Content and Pcb Concentrations in Planktonic Food Webs. *Ecology*. 82, 4 (2001), 1078–1088. DOI:https://doi.org/10.1890/0012-9658(2001)082[1078:TEOLTO]2.0.CO;2.

[8]   Bligh, E.G. and Dyer, W.J. 1959. A Rapid Method of Total Lipid Extraction and Purification. *Canadian Journal of Biochemistry and Physiology*. 37, 8 (Aug. 1959), 911–917. DOI:https://doi.org/10.1139/o59-099.

[9]   Booij, K. et al. 2007. Chapter 7 Theory, modelling and calibration of passive samplers used in water monitoring. *Comprehensive Analytical Chemistry*. R. Greenwood et al., eds. Elsevier. 141–169.

[10] Booij, K. et al. 2002. Spiking of performance reference compounds in low density polyethylene and silicone passive water samplers. *Chemosphere*. 46, 8 (Mar. 2002), 1157–1161. DOI:https://doi.org/10.1016/S0045-6535(01)00200-4.

[11] Booij, K. et al. 2003. Temperature-Dependent Uptake Rates of Nonpolar Organic Compounds by Semipermeable Membrane Devices and Low-Density Polyethylene Membranes. *Environmental Science & Technology*. 37, 2 (Jan. 2003), 361–366. DOI:https://doi.org/10.1021/es025739i.

[12] Booij, K. and Smedes, F. 2010. An Improved Method for Estimating in Situ Sampling Rates of Nonpolar Passive Samplers. *Environmental Science & Technology*. 44, 17 (Sep. 2010), 6789–6794. DOI:https://doi.org/10.1021/es101321v.

[13] Borgå, K. et al. 2005. Bioaccumulation Factors for PCBs Revisited. *Environmental Science & Technology*. 39, 12 (Jun. 2005), 4523–4532. DOI:https://doi.org/10.1021/es050376i.

[14] Campfens, J. and Mackay, D. 1997. Fugacity-Based Model of PCB Bioaccumulation in Complex Aquatic Food Webs. *Environmental Science & Technology*. 31, 2 (Feb. 1997), 577–583. DOI:https://doi.org/10.1021/es960478w.

[15] Choi, Y. et al. 2013. Polyethylene–Water Partitioning Coefficients for Parent- and Alkylated-Polycyclic Aromatic Hydrocarbons and Polychlorinated Biphenyls. *Environmental Science & Technology*. 47, 13 (Jul. 2013), 6943–6950. DOI:https://doi.org/10.1021/es304566v.

[16] Connolly and Pederson 1988. A thermodynamic based evaluatiion of organic chemical accumulation in aquatic organisms. (1988).

[17] Endo, S. et al. 2011. Capacities of Membrane Lipids to Accumulate Neutral Organic Chemicals. *Environmental Science & Technology*. 45, 14 (Jul. 2011), 5912–5921. DOI:https://doi.org/10.1021/es200855w.

[18] Fernandez, L.A. et al. 2009. Using Performance Reference Compounds in Polyethylene Passive Samplers to Deduce Sediment Porewater Concentrations for Numerous Target Chemicals. *Environmental Science and Technology*. 43, (Dec. 2009), 8888–8894. DOI:https://doi.org/10.1021/es901877a.

[19] Geisler, A. et al. 2012. Partitioning of Organic Chemicals to Storage Lipids: Elucidating the Dependence on Fatty Acid Composition and Temperature. *Environmental Science & Technology*. 46, 17 (Sep. 2012), 9519–9524. DOI:https://doi.org/10.1021/es301921w.

[20] Gobas, F.A.P.C. 1993. A model for predicting the bioaccumulation of hydrophobic organic chemicals in aquatic food-webs: application to Lake Ontario. *Ecological Modelling*. 69, 1–2 (Sep. 1993), 1–17. DOI:https://doi.org/10.1016/0304-3800(93)90045-T.

[21] Greenberg, A.E. et al. 1992. *Standard Methods for the Examination of Water and Wastewater*. American Public Health Association.

[22] Gschwend, P. and Palaia, K. 2015. *Passive PE Sampling in Support of In Situ Remediation of Contaminated Sediments:*. Defense Technical Information Center.

[23] Gustafsson, C. and Gschwend, P.M. 1997. Aquatic colloids: Concepts, definitions, and current challenges. *Limnology and Oceanography*. 42, 3 (May 1997), 519–528. DOI:https://doi.org/10.4319/lo.1997.42.3.0519.

[24] Hawker, D.W. and Connell, D.W. 1988. Octanol-water partition coefficients of polychlorinated biphenyl congeners. *Environmental Science & Technology*. 22, 4 (Apr. 1988), 382–387. DOI:https://doi.org/10.1021/es00169a004.

[25] Hayduk, W. and Laudie, H. 1974. Prediction of diffusion coefficients for nonelectrolytes in dilute aqueous solutions. *AIChE Journal*. 20, 3 (May 1974), 611–615. DOI:https://doi.org/10.1002/aic.690200329.

[26] Jakobsen, H.H. and Markager, S. 2016. Carbon-to-chlorophyll ratio for phytoplankton in temperate coastal waters: Seasonal patterns and relationship to nutrients: C:Chl for phytoplankton in temperate coastal waters. *Limnology and Oceanography*. 61, 5 (Sep. 2016), 1853–1868. DOI:https://doi.org/10.1002/lno.10338.

[27] KABAM Version 1.0 User's Guide and Technical Documentation: 2015. *https://www.epa.gov/pesticide-science-and-assessing-pesticide-risks/kabam-version-10-users-guide-and-technical*. Accessed: 2019-08-27.

[28] Liu, H. et al. 2016. Effect of Diatom Silica Content on Copepod Grazing, Growth and Reproduction. *Frontiers in Marine Science*. 3, (2016). DOI:https://doi.org/10.3389/fmars.2016.00089.

[29] Lohmann, R. 2012. Critical Review of Low-Density Polyethylene's Partitioning and Diffusion Coefficients for Trace Organic Contaminants and Implications for Its Use As a Passive Sampler. *Environmental Science & Technology*. 46, 2 (Jan. 2012), 606–618. DOI:https://doi.org/10.1021/es202702y.

[30] Lourenço, S.O. et al. 1998. Distribution of Intracellular Nitrogen in Marine Microalgae: Basis for the Calculation of Specific Nitrogen-to-Protein Conversion Factors. *Journal of Phycology*. 34, 5 (1998), 798–811. DOI:https://doi.org/10.1046/j.1529-8817.1998.340798.x.

[31] Lourenço, S.O. et al. 2004. Distribution of intracellular nitrogen in marine microalgae: Calculation of new nitrogen-to-protein conversion factors. *European Journal of Phycology*. 39, 1 (Feb. 2004), 17–32. DOI:https://doi.org/10.1080/0967026032000157156.

[32] Menzel, D.W. and Vaccaro, R.F. 1964. The Measurement of Dissolved Organic and Particulate Carbon in Seawater1. *Limnology and Oceanography*. 9, 1 (1964), 138–142. DOI:https://doi.org/10.4319/lo.1964.9.1.0138.

[33] Nizzetto, L. et al. 2012. Biological Pump Control of the Fate and Distribution of Hydrophobic Organic Pollutants in Water and Plankton. *Environmental Science & Technology*. 46, 6 (Mar. 2012), 3204–3211. DOI:https://doi.org/10.1021/es204176q.

[34] Oliver, B.G. and Niimi, A.J. 1988. Trophodynamic analysis of polychlorinated biphenyl congeners and other chlorinated hydrocarbons in the Lake Ontario ecosystem. *Environ. Sci. Technol. Environmental Science & Technology*. 22, 4 (1988), 388–397.

[35] Rusina, T.P. et al. 2010. Diffusion coefficients of polychlorinated biphenyls and polycyclic aromatic hydrocarbons in polydimethylsiloxane and low-density polyethylene polymers. *Journal of Applied Polymer Science*. 116, 3 (2010), 1803–1810. DOI:https://doi.org/10.1002/app.31704.

[36] Schulz, D.E. et al. 1989. Complete characterization of polychlorinated biphenyl congeners in commercial Aroclor and Clophen mixtures by multidimensional gas chromatography-electron capture detection. *Environmental Science & Technology*. 23, 7 (Jul. 1989), 852–859. DOI:https://doi.org/10.1021/es00065a015.

[37] Schwarzenbach, R.P. et al. 2016. *Environmental Organic Chemistry*. John Wiley & Sons.

[38] Skoglund, R.S. et al. 1996. A Kinetics Model for Predicting the Accumulation of PCBs in Phytoplankton. *Environmental Science & Technology*. 30, 7 (Jan. 1996), 2113–2120. DOI:https://doi.org/10.1021/es950206d.

[39] Stange, K. and Swackhamer, D.L. 1994. Factors affecting phytoplankton species-specific differences in accumulation of 40 polychlorinated biphenyls (PCBs). *Environmental Toxicology and Chemistry*. 13, 11 (Nov. 1994), 1849–1860. DOI:https://doi.org/10.1002/etc.5620131117.

[40] Swackhamer, D.L. 1991. Bioaccumulation of toxic hydrophobic organic compounds at the primary trophic level. *J Environ Sci (China)*. 3, 3 (1991), 15–21.

[41] Swackhamer, D.L. and Skoglund, R.S. 1993. Bioaccumulation of PCBs by algae: Kinetics versus equilibrium. *Environmental Toxicology and Chemistry*. 12, 5 (May 1993), 831–838. DOI:https://doi.org/10.1002/etc.5620120506.

[42] Tcaciuc, A.P. et al. 2015. Modeling the transport of organic chemicals between polyethylene passive samplers and water in finite and infinite bath conditions: Modeling PE-water transfer in finite and infinite baths. *Environmental Toxicology and Chemistry*. 34, 12 (Dec. 2015), 2739–2749. DOI:https://doi.org/10.1002/etc.3128.

[43] Tcaciuc, A.P. 2015. *Using passive samplers to assess bioavailability, toxicity, and reactivity of hydrophobic organic chemicals (HOCs)*. Massachusetts Institute of Technology.

[44] Thomann, R.V. 1989. Bioaccumulation model of organic chemical distribution in aquatic food chains. *Environmental Science & Technology*. 23, 6 (Jun. 1989), 699–707. DOI:https://doi.org/10.1021/es00064a008.

[45] Two complementary sides of bioavailability: Accessibility and chemical activity of organic contaminants in sediments and soils: 2006. *http://setac.onlinelibrary.wiley.com/doi/abs/10.1897/05-458R.1*. Accessed: 2019-07-16.

33

[46] Van Nieuwerburgh, L. et al. 2004. Growth and C:N:P ratios in copepods grazing on N- or Si-limited phytoplankton blooms. *Biology of the Baltic Sea* (2004), 57–72.

[47] Wade, T.L. et al. 1993. Sampling and analytical methods of the National Status and Trends program National Benthic Surveillance and Mussel Watch Projects, 1984-1992. (1993), II.41-42.

[48] Whipple, G.C. and Parker, H.N. 1902. On the Amount of Oxygen and Carbonic Acid Dissolved in Natural Waters and the Effect of These Gases upon the Occurrence of Microscopic Organisms. *Transactions of the American Microscopical Society*.

[49] Yaws, C.L. 2009. *Transport Properties of Chemicals and Hydrocarbons: Viscosity, Thermal Conductivity, and Diffusivity for more than 7800 Hydrocarbons and Chemicals, Including C1 to C100 Organics and Ac to Zr Inorganics*. Elsevier Science.

[50] Zhang, L. et al. 2015. Simulation of Observed PCBs and Pesticides in the Water Column during the North Atlantic Bloom Experiment. *Environmental Science & Technology*. 49, 23 (Dec. 2015), 13760–13767. DOI:https://doi.org/10.1021/acs.est.5b00223.

[51] Zhang, L. and Lohmann, R. 2010. Cycling of PCBs and HCB in the Surface Ocean-Lower Atmosphere of the Open Pacific. *Environmental Science & Technology*. 44, 10 (May 2010), 3832–3838. DOI:https://doi.org/10.1021/es9039852.

Supplementary Figures and Tables

Figure S1. Estimation of silica. 5 ml of phytoplankton sample filtered on 45 mm Whatman filters (left) were baked at 450 C for 12 h. The remaining inorganic solid was off-white and shiny (right).
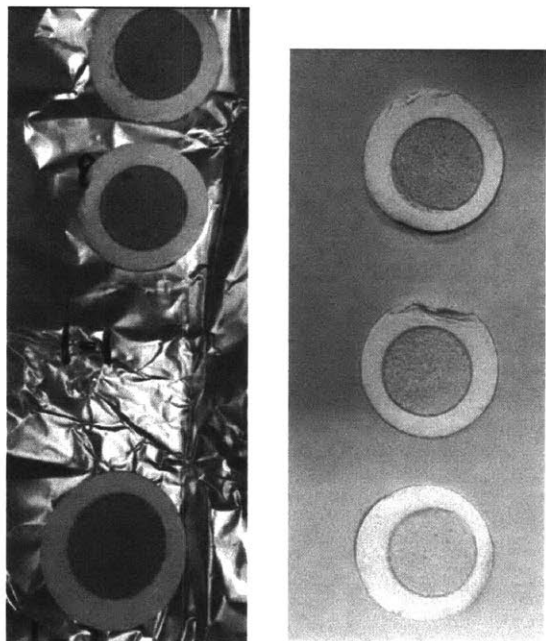
Figure S2. Angela Cacciola (MIT) samples zooplankton off the boat in Lake Cochituate, MA. July 26, 2017.

Figure S3 Zooplankton on Nitex filter
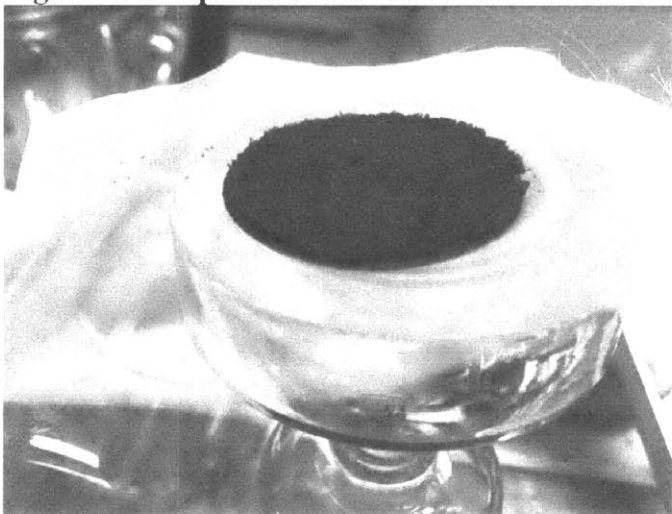
Figure S4 Phytoplankton (left) and zooplankton (right) DCM extracts
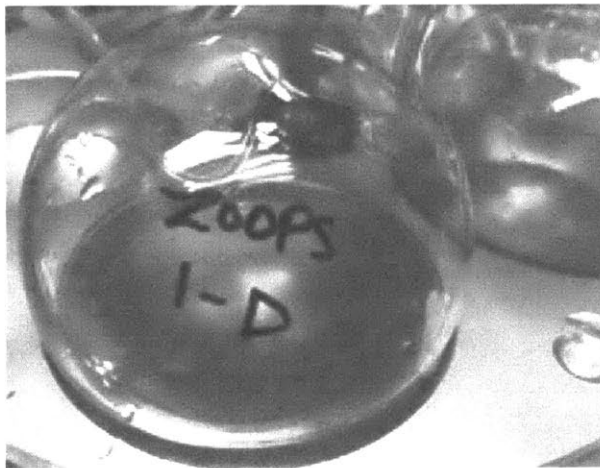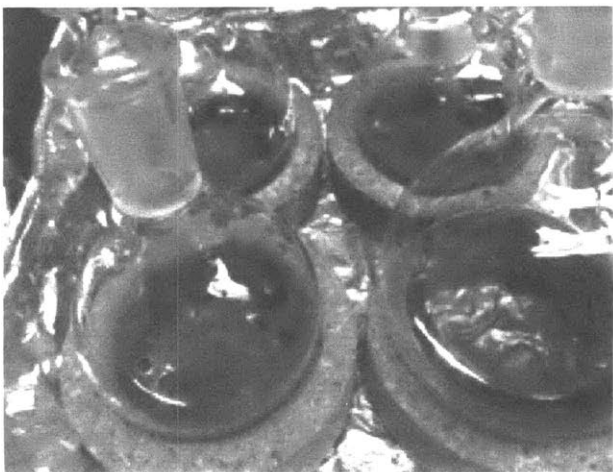
Table S1. Lake Cochituate PE Sites: Fall 2015, Fall 2016, Spring 2017

Sampling	Water Temp	PE Site	Latitude Degrees, minutes, seconds North	Longitude West
Fall 2016	12'C	1	42° 17' 12.264"	71° 21' 36.504"
		2	42° 17' 26.124"	71° 21' 31.1394"
October 16 – Dec 3		2A	42° 17' 19.608"	71° 21' 39.0234"
		3	42° 17' 16.2594"	71° 21' 28.3674"
		4A	42° 17' 05.352"	71° 21' 32.4354"
		5A	42° 17' 05.1354"	71° 22' 04.6194"
		7	42° 17' 12.444"	71° 22' 18.0114"
		8	42° 17' 40.884"	71° 22' 17.2194"
		9	42° 17' 51.0714"	71° 22' 00.696"
		10	42° 17' 16.2594"	71° 21' 53.316"
Spring/Summer 2017	24.7'C (July 21)	1	42° 17' 11.975"	71° 21' 36.935"
		2	42° 17' 23.4234"	71° 21' 36.6114"
		3	42° 17' 16.044"	71° 21' 28.008"
May 23 - July 17		4	42° 17' 07.2954"	71° 21' 31.176"
		5	42° 17' 02.4714"	71° 21' 34.5234"
		7	42° 17' 22.020"	71° 22' 26.148"
		8	42° 17' 40.884"	71° 22' 17.0394"
		9	42° 17' 51.252"	71° 22' 01.0914"
		10	42° 17' 16.548"	71° 21' 53.7114"

Figure S5 John MacFarlane from MIT deploys a sediment-water interface PE frame and and attached water column PE mesh. May 23, 2017. Lake Cochituate, Natick, MA.

Figure S6 Passive Samplers
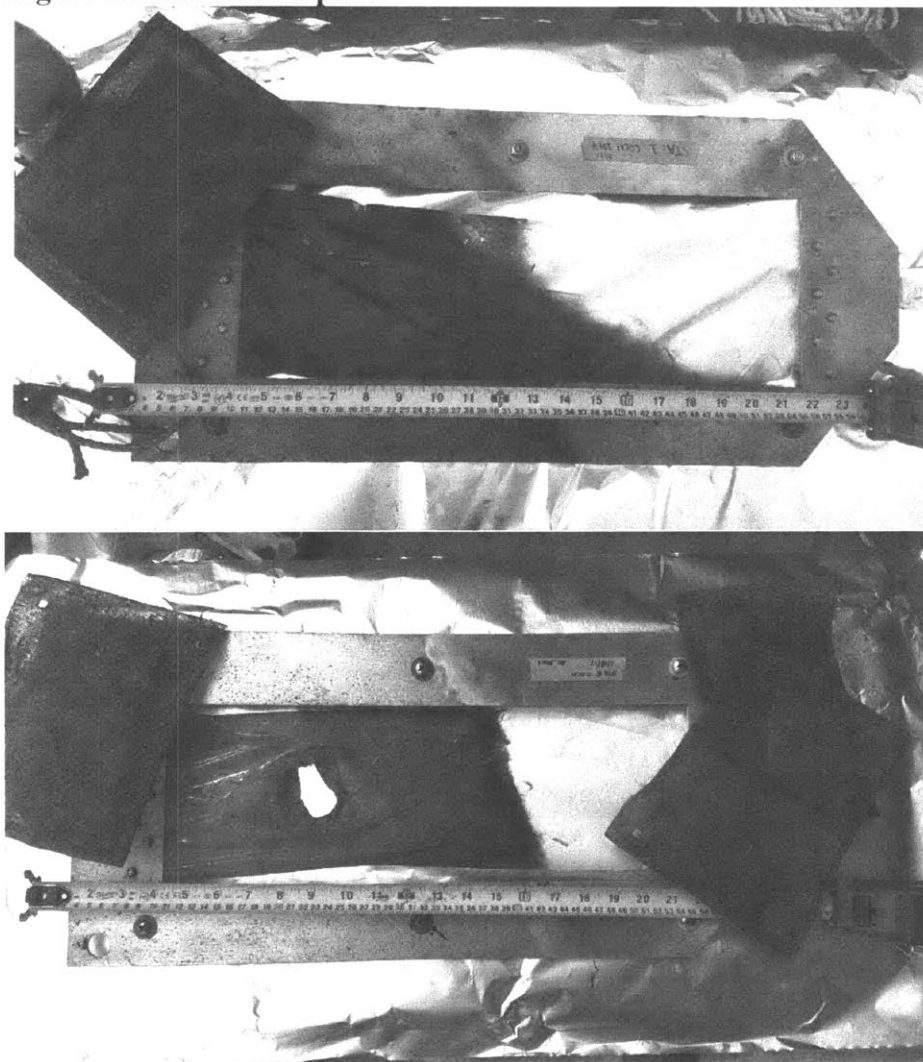
Table S2 GCMS Response Factors

Congener	PE Retention Time (min)	Relative Retention Time (PCB 101)	MIT-AC Response Factor (area/pg) 2017 PE	2017 Plankton	2016 Plankton
PCB 8	13.40	0.508	7255	4738	4942
PCB 18	15.24	0.577	3841	2678	3142
PCB 28	17.93	0.679	4784	3032	3395
PCB 52	19.97	0.757	3827	2601	3061
PCB 44	21.31	0.807	3325	2312	2771
PCB 66	24.62	0.933	3952	2237	2754
PCB 77	29.91	1.133	2886	1998	1794
PCB 101	26.39	1.000	3520	2455	2848
PCB 118	31.94	1.210	3813	2433	2730
PCB 105	34.26	1.298	3369	2227	2439
PCB 126	37.82	1.433	2325	1412	1689
PCB 153	33.86	1.283	3253	2273	2606
PCB 138	36.41	1.379	2868	1937	2208
PCB 128	38.97	1.476	2392	1775	1863
PCB 187	37.84	1.434	2629	1896	2043
PCB 180	43.14	1.635	2313	1798	1860
PCB 170	45.96	1.741	2033	1606	1596
PCB 195	50.33	1.907	2084	1745	1504
PCB 206	56.30	2.133	2088	2074	1384
PCB 209	59.38	2.250	2467	2065	1637
PCB 39	19.99	0.718	4308	2706	2592
PCB 104	25.23	0.907	3975	2499	2528
PCB 55	20.91	0.751	4727	3328	1875
PCB 150	27.24	0.979	3288	2242	1831
PCB 188	32.92	1.183	3310	2289	1250
^{13}CPCB 19	14.15	0.54	3744	2572	2343
^{13}CPCB 52	19.95	0.76	2783	2407	2424
^{13}CPCB 105	34.24	1.30	2985	2147	3423
^{13}CPCB 167	39.45	1.49	2930	2043	2912
^{13}CPCB 194	45.93	1.74	1905	1519	2335
^{13}CPCB 32	16.23	0.615	5609		
^{13}CPCB 54	16.95	0.642	3561		
^{13}CPCB 47	20.39	0.773	3285		
^{13}CPCB 101	26.37	0.999	3638		
^{13}CPCB 111	28.47	1.079	4263		
^{13}CPCB 138	36.38	1.378	3140		
^{13}CPCB 178	36.96	1.400	2495		

Table S3 Protein and Lipid Partition Coefficients

Congener	Kmlip 25'c	SD log Kmlip	log Kmlip 20'C	log Kmlip 12'C	log Kprotein 25'C	SD log Kprotein
PCB 8	5.27	0.21	5.33	5.43	3.45	0.00
PCB 18	5.91	0.22	5.97	6.09	3.97	0.04
PCB 28	5.59	0.20	5.67	5.80	3.73	0.00
PCB 52	6.37	0.22	6.45	6.59	4.37	0.06
PCB 44	6.37	0.22	6.46	6.61	4.37	0.06
PCB 66	6.50	0.21	6.59	6.74	4.53	0.04
PCB 77	6.33	0.19	6.41	6.56	4.42	0.00
PCB 101	6.80	0.22	6.89	7.04	4.75	0.07
PCB 118	6.90	0.21	6.99	7.16	4.89	0.05
PCB 105	6.90	0.21	7.00	7.17	4.89	0.05
PCB 126	7.01	0.20	7.12	7.28	5.05	0.03
PCB 153	7.22	0.23	7.32	7.49	5.13	0.09
PCB 138	7.22	0.23	7.33	7.50	5.13	0.09
PCB 128	7.22	0.23	7.33	7.52	5.13	0.09
PCB 187	7.23	0.24	7.34	7.53	5.09	0.10
PCB 180	7.65	0.24	7.76	7.95	5.51	0.10
PCB 170	7.65	0.24	7.76	7.96	5.51	0.10
PCB 195	8.26	0.26	8.38	8.57	6.01	0.16
PCB 206	8.29	0.26	8.42	8.63	6.03	0.15
PCB 209	8.79	0.28	8.91	9.13	6.41	0.20

Table S4 Octanol Water and PE Partition Coefficients

Congener	log Kow	delta How	log Kpew 25'C	log Kpew 20'C	SD log Kpew 20'C	log Kpew 12'C
PCB 8	5.07	-20	4.54	4.60	0.03	4.70
PCB 18	5.24	-23	4.77	4.84	0.03	4.95
PCB 28	5.67	-26	5.18	5.26	0.02	5.39
PCB 52	5.84	-28	5.35	5.43	0.02	5.57
PCB 44	5.75	-29	5.28	5.37	0.03	5.52
PCB 66	6.20	-30	5.85	5.94	0.03	6.09
PCB 77	6.36	-29	5.70	5.79	0.03	5.94
PCB 101	6.38	-31	6.10	6.19	0.03	6.34
PCB 118	6.74	-32	6.32	6.42	0.03	6.58
PCB 105	6.65	-34	6.34	6.44	0.07	6.61
PCB 126	6.89	-34	6.48	6.58	*	6.75
PCB 153	6.92	-34	6.71	6.81	0.06	6.98
PCB 138	6.83	-35	6.55	6.66	0.04	6.84
PCB 128	6.74	-37	6.41	6.52	0.01	6.70
PCB 187	7.17	-37	6.75	6.86	*	7.05
PCB 180	7.36	-38	7.09	7.20	0.01	7.39
PCB 170	7.27	-39	6.85	6.96	*	7.16
PCB 195	7.56	-39	7.26	7.38	0.14	7.57
PCB 206	8.09	-43	7.43	7.56	0.28	7.78
PCB 209	8.18	-42	7.77	7.89	*	8.10
[13C]PCB 32	5.44	-25	4.86	4.93	0.03	5.06
[13C]PCB 54	5.85	-28	5.43	5.52	*	5.66
[13C]PCB 47	5.84	-29	5.42	5.51	*	5.65
[13C]PCB 101	6.38	-31	6.10	6.19	*	6.34
[13C]PCB 111	**6.76**	-30	6.35	6.44	*	6.59
[13C]PCB 138	**6.83**	-35	6.55	6.66	0.04	6.84
[13C]PCB 178	**7.14**	-35	6.89	6.99	0.06	7.16

Table S5 Diffusion Coefficients

Congener	Vm	log Dw 25'C	log Dw 12'C	log Dw 25'C
PCB 8		-5.10	-5.26	-5.21
PCB 18		-5.11	-5.27	-5.22
PCB 28		-5.10	-5.26	-5.21
PCB 52		-5.12	-5.28	-5.24
PCB 44		-5.12	-5.28	-5.24
PCB 66		-5.14	-5.30	-5.25
PCB 77		-5.14	-5.30	-5.25
PCB 101		-5.14	-5.30	-5.26
PCB 118		-5.16	-5.32	-5.27
PCB 105		-5.16	-5.32	-5.27
PCB 126		-5.17	-5.33	-5.28
PCB 153		-5.16	-5.32	-5.27
PCB 138		-5.16	-5.32	-5.27
PCB 128		-5.16	-5.32	-5.27
PCB 187		-5.15	-5.31	-5.27
PCB 180		-5.18	-5.34	-5.29
PCB 170		-5.18	-5.34	-5.29
PCB 195		-5.19	-5.35	-5.31
PCB 206		-5.19	-5.35	-5.31
PCB 209		-5.20	-5.36	-5.32
^{13}CPCB 32		-5.10	-5.26	-5.21
^{13}CPCB 54		-5.10	-5.26	-5.20
^{13}CPCB 47		-5.12	-5.28	-5.24
^{13}CPCB 101		-5.14	-5.30	-5.26
^{13}CPCB 111		-5.16	-5.32	-5.27
^{13}CPCB 138		-5.16	-5.32	-5.27
^{13}CPCB 178		-5.16	-5.32	-5.28

45

Figure S7 Zooplankton and detritus among phytoplankton diatoms
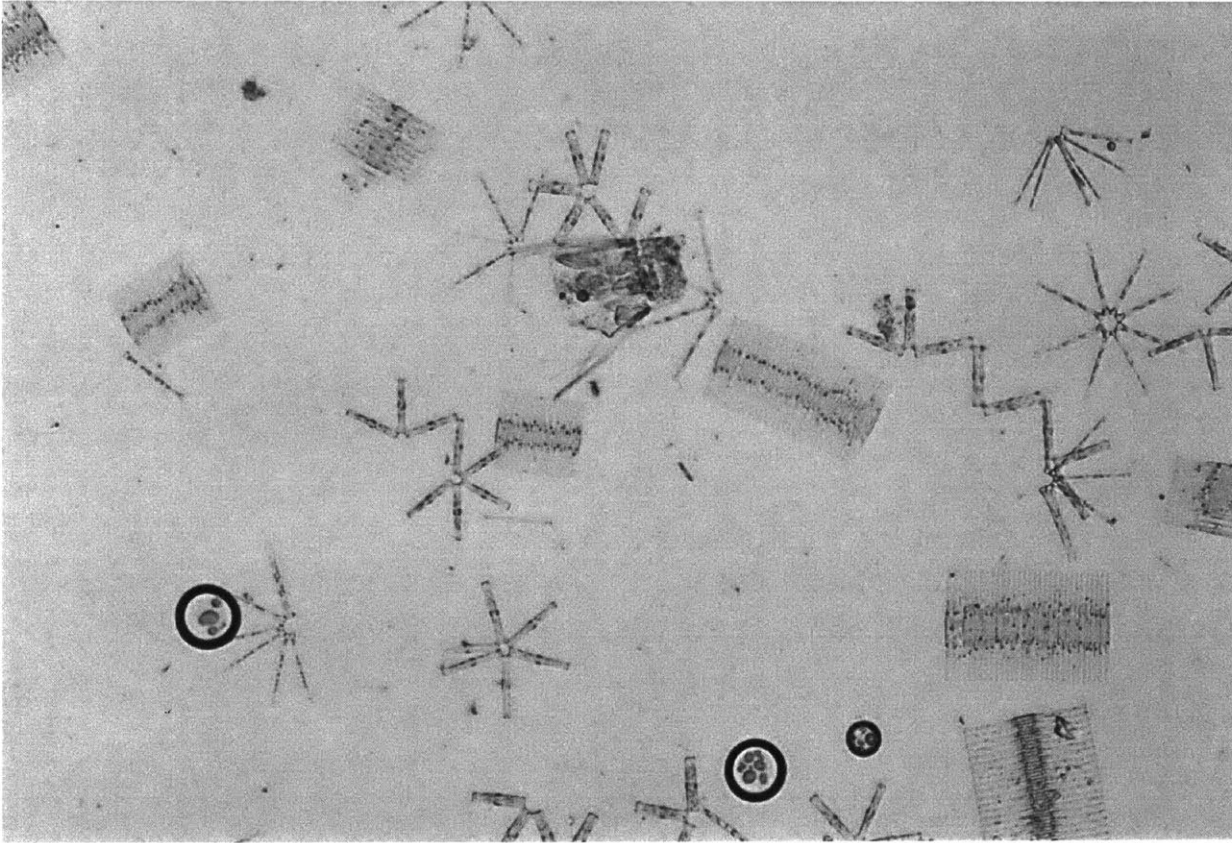
Table S6 Lipid partitioning compared to protein and carbohydrate partitioning

Target Congeners EPA 20	Kmlip/Kslip	Kmlip/Kprot	Kmlip/Kcarb
PCB 8	1	70	2000
PCB 18	4	90	8000
PCB 28	1	70	2000
PCB 52	3	100	8000
PCB 44	3	100	9000
PCB 66	2	90	6000
PCB 77	1	80	3000
PCB 101	2	110	8000
PCB 118	1	100	6000
PCB 105	1	100	7000
PCB 126	1	90	6000
PCB 153	2	120	9000
PCB 138	2	120	10000
PCB 128	1	120	12000
PCB 187	1	140	6000
PCB 180	1	140	11000
PCB 170	1	140	13000
PCB 195	2	180	33000
PCB 206	1	180	14000
PCB 209	2	240	39000

Kslip - (Geisler, Endo, and Goss 2012)

Kmlip -(Endo, Escher, and Goss 2011)

Kprot - (Endo, Bauerfeind, and Goss 2012)

Kcarb - (Hung, Lin, and Chiou 2010)

Table S7 Surrogate and injection recoveries PE

Congener	Cl #	2017 PE Extract volume (µl)														
		0-5 cm overlying water						1 m water column					Water column t=0			SWI t=0
		S1	S3	S4	S8	S9	S10	S1	S2	S4	S8	S10	#3	#9	Field blank	Field blank
PCB 39	3	14	I	I	I	I	18	I	I	I	I	I	31	I	I	o
PCB 55	4	15	15	6	17	20	22	43	40	6	13	13	30	27	31	22
PCB 104	5	17	20	9	23	26	28	70	57	15	17	25	35	32	37	28
PCB 150	6	18	20	8	23	25	28	72	56	15	17	24	36	32	37	28
PCB 188	7	18	19	8	22	24	27	71	56	15	16	24	32	30	34	26
Average		17	19	8	21	24	26	64	52	13	16	21	33	30	35	26
RSD 4-7Cl		10%	13%	12%	14%	12%	12%	22%	15%	34%	13%	27%	8%	8%	8%	11%

I = peak interference

Congener	#Cl	2016 PE Extract volume (µl)																
		0-5 cm overlying water						1 m water column						t=0			Field blank WC	Field Blank SWI
		S1	S2	S3	S7	S8	S10	S1	S2	S3	S8	S9	S10	WC	SWIa	SWIb		
PCB 39	3	69	51	64	58	67	55	42	40	46	66	65	92	65	58	78	57	99
PCB 104	5	60	48	53	50	54	43	33	37	37	53	49	54	44	42	44	42	45
PCB 55	4	59	47	51	49	52	38	34	37	38	49	46	43	41	48	51	48	52
PCB 150	6	57	47	51	50	51	42	35	38	38	51	48	55	44	46	47	45	47
PCB 188	7	60	48	54	52	56	45	38	41	44	55	50	59	44	46	48	45	48
Average 4-7 Cl		61	48	55	52	56	45	36	39	41	55	52	61	43	45	47	45	48
RSD		8%	3%	10%	7%	11%	14%	10%	5%	10%	12%	15%	30%	3%	5%	6%	5%	5%

	Congener	Average % Surrogate Recovery 2016 and 2017 PE								
		0-5 cm			WC			T=0		
		AVG	SD	RSD	AVG	SD	RSD	AVG	SD	RSD
2016 PE	13C PCB 19	**88%**	8%	9%	**91%**	14%	15%	**120%**	32%	26%
	13C PCB 52	**73%**	9%	13%	**75%**	7%	10%	**86%**	5%	6%
	13C PCB 105	**94%**	9%	10%	**97%**	11%	11%	**90%**	7%	8%
	13C PCB167	**102%**	9%	9%	**98%**	9%	10%	**91%**	16%	17%
	13C PCB 194	**91%**	10%	11%	**96%**	9%	10%	**117%**	7%	6%
2017 PE	13C PCB 19	39%	8%	20%	27%	17%	62%	**65%**	16%	24%
	13C PCB 52	61%	12%	20%	58%	55%	53%	**84%**	17%	20%
	13C PCB 105	120%	22%	18%	125%	123%	126%	**136%**	26%	19%
	13C PCB167	110%	20%	18%	113%	112%	119%	**131%**	26%	20%
	13C PCB 194	103%	18%	17%	109%	107%	104%	**117%**	24%	21%

Table S8 PRC concentrations at t = 0

Congener	Cl#	Average CPE, t=0 (ng/g)						
		17PEWC (n=3)			17PE05 (n=1)	16PEWC and 16PE05 (n=5)		
		AVG	SD	RSD	n=1	Average	SD	RSD
[13C]PCB 32	3	29	6	19%	oversaturated	75	27	36%
[13C]PCB 54	4	12	1	7%	oversaturated	94	32	34%
[13C]PCB 47	4	48	2	4%	53	116	25	21%
[13C]PCB 101	5	45	2	5%	34	73	15	20%
[13C]PCB 111	5	56	3	5%	24	55	17	30%
[13C]PCB 138	6	54	3	5%	24	56	13	22%
[13C]PCB 178	7	60	3	5%	17	34	10	30%

Table S9 Measured and fitted f$_{pe}$

2016 0-5 cm PE

	S1 Meas	Fit	S2 Meas	Fit	S2A Meas	Fit	S3 Meas	Fit	S7 Meas	Fit	S8 Meas	Fit	S10 Meas	Fit
PRC 32	0.04	0.02	0.22	0.03	0.03	0.00	0.02	0.00	0.07	0.02	0.03	0.01	0.11	0.00
PRC 54	0.02	0.38	0.21	0.41	0.06	0.17	0.02	0.22	0.08	0.36	0.04	0.26	0.15	0.15
PRC 47	0.33	0.40	0.57	0.42	0.41	0.19	0.43	0.24	0.65	0.38	0.51	0.28	1.69	0.17
PRC 101	0.45	0.84	0.84	0.85	0.56	0.72	0.59	0.76	1.51	0.83	0.76	0.78	0.00	0.70
PRC 111	0.37	0.91	1.27	0.91	0.93	0.84	0.92	0.86	7.17	0.90	0.87	0.87	1.86	0.83
PRC 138	0.37	0.95	1.16	0.95	0.71	0.90	0.92	0.92	3.38	0.94	0.88	0.93	1.97	0.90
PRC 178	0.44	0.97	1.98	0.98	1.13	0.95	1.46	0.96	0.00	0.97	1.24	0.97	0.00	0.95
BLT um		451		487		248		289		432		328		232
sum RMSE		0.28		0.09		0.09		0.11		0.15		0.10		0.01

2016 WC PE

	S1 Meas	Fit	S2 Meas	Fit	S2A Meas	Fit	S3 Meas	Fit	S7 Meas	Fit	S8 Meas	Fit	S9 Meas	Fit	S10 Meas	Fit
PRC 32	0.03	0.01	0.06	0.01	0.06	0.01	0.02	0.01	0.06	0.02	0.06	0.02	0.18	0.10	0.06	0.01
PRC 54	0.04	0.26	0.09	0.34	0.10	0.34	0.03	0.29	0.09	0.37	0.09	0.36	0.37	0.56	0.10	0.34
PRC 47	0.38	0.28	0.49	0.36	0.45	0.36	0.40	0.30	0.48	0.38	0.47	0.38	0.62	0.58	0.48	0.36
PRC 101	0.97	0.78	0.82	0.82	0.92	0.82	0.90	0.79	0.99	0.83	0.91	0.83	0.95	0.90	0.96	0.82
PRC 111	0.96	0.87	0.73	0.90	1.04	0.90	1.16	0.88	1.11	0.90	1.06	0.90	0.86	0.94	1.23	0.90
PRC 138	1.03	0.93	0.76	0.94	1.07	0.94	1.24	0.93	1.09	0.94	1.05	0.94	0.80	0.97	1.15	0.94
PRC 178	1.34	0.97	0.93	0.97	1.36	0.97	1.74	0.97	1.49	0.97	1.47	0.97	0.97	0.98	1.83	0.97
BLT um		451		408		408		351		437		429		759		404
sum RMSE		0.06		0.08		0.07		0.08		0.09		0.08		0.04		0.07

52

2017 0-5 cm PE

	S1		S3		S4		S8		S9		S10	
	Meas	Fit	Meas	Fit	Meas	Fit	Meas	Fit	Meas	Fit	Meas	Fit
PRC 47	0.15	0.00	0.02	0.00	0.15	0.00	0.14	0.00	0.26	0.00	0.48	0.27
PRC 101	0.30	0.21	0.07	0.01	0.24	0.13	0.32	0.22	0.32	0.14	0.61	0.77
PRC 111	0.49	0.44	0.12	0.09	0.36	0.33	0.49	0.45	0.32	0.35	0.74	0.87
PRC 138	0.56	0.61	0.17	0.22	0.44	0.51	0.64	0.61	0.39	0.53	1.03	0.92
PRC 178	0.85	0.79	0.24	0.50	0.59	0.73	0.82	0.80	0.41	0.74	0.82	0.96
del um		151		51		112		154		117		909
sum RMSE		0.0360		0.0757		0.0623		0.0305		0.2267		0.0897

2017 WC PE

	S1		S2		S4		S8		S10	
	Meas	Fit	Meas	Fit	Meas	Fit	Meas	Fit	Meas	Fit
PRC 32	0.00	0.00	0.00	0.00	0.00	0.00	0.02	0.00	0.08	0.00
PRC 54	0.00	0.00	0.00	0.00	0.04	0.00	0.00	0.02	0.05	0.01
PRC 47	0.08	0.00	0.11	0.00	0.17	0.00	0.23	0.02	0.20	0.01
PRC 101	0.26	0.17	0.34	0.18	0.40	0.32	0.50	0.44	0.46	0.40
PRC 111	0.44	0.39	0.50	0.40	0.57	0.54	0.65	0.65	0.63	0.62
PRC 138	0.54	0.56	0.58	0.57	0.69	0.69	0.74	0.77	0.73	0.74
PRC 178	0.64	0.77	0.68	0.77	0.78	0.84	0.81	0.88	1.14	0.87
del um		130.46		136.15		202.75		283.33		255.46
sum		0.0344		0.0553		0.0409		0.0522		0.0419
RMSE										

Table S11 $C_{phytoplankton}$ and $C_{zooplankton}$ (ng/g lipid)

Congener	# Cl	2016 Phytoplankton		2017 Phytoplankton		2017 Zooplankton	
		Site 1	Site	Site 1	Site 8	Site 1	Site 8
PCB 8	2			18.0	35.1	14.3	
PCB 18	3		12.3	30.7	53.6	69.6	33.4
PCB 28	3	51.0		107.4	165.6	405.6	187.6
PCB 52	4	183.0	56.3	72.0	29.6	276.0	105.6
PCB 44	4	22.8	28.6	22.9	11.9	52.3	25.2
PCB 66	4	74.6	36.3	19.6	13.9	98.2	50.8
PCB 77	4			10.6	15.6	24.4	
PCB 101	5	222.0	69.3	84.5	49.2	423.2	271.4
PCB 118	5	75.2	37.9	28.6	18.0	158.4	84.6
PCB 105	5		12.2	13.5	8.3	49.2	28.0
PCB 126	5						
PCB 153	6	492.2	151.3	139.1	48.8	914.6	482.9
PCB 138	6	277.2	72.2	75.6	31.5	544.5	238.3
PCB 128	6	34.8		14.4	5.9	61.4	28.1
PCB 187	7	209.1	36.5	71.2	21.2	413.9	193.8
PCB 180	7	343.1	92.7	115.4	34.0	616.1	248.1
PCB 170	7	156.5	29.8	57.9	15.6	283.3	97.2
PCB 195	8			15.2	3.0	65.4	20.5
PCB 206	9			11.9		30.9	12.8
PCB 209	10			12.0	4.5	28.7	12.1

Table S12 C_{pe}, measured (ng PCB/g PE)

Congener	# Cl	2016 0-5 cm PE								2016 WC PE						
		S1	S2	S2A	S3	S7	S8	S9	S10	S1	S2A	S2	S3	S8	S9	S10
PCB 8	2															
PCB 18	3	0.2	0.5	0.3	0.1			0.6	0.2	0.3	0.2	0.2	0.2	0.1	0.1	0.2
PCB 28	3	0.9	2.4	1.0	0.9	0.5	0.5	2.5	0.7	0.9	0.9	0.8	0.5	0.5	0.2	0.6
PCB 52	4	2.8	4.0	2.2	2.5	0.8	1.0	5.7	2.4	2.2	2.0	2.3	0.9	0.7	0.4	1.2
PCB 44	4	0.5	0.6	0.8	0.6	0.2	0.3	1.1	0.4	0.4	0.4	0.4	0.2	0.2	0.1	0.2
PCB 66	4	0.8	0.9	1.3	1.0	0.4	0.5	2.2	0.5	0.5	0.6	0.6	0.3	0.3	0.1	0.3
PCB 77	4															
PCB 101	5	2.1	1.7	2.6	1.7	0.7	1.0	4.0	1.3	1.0	1.3	1.2	0.6	0.5	0.2	1.0
PCB 118	5	1.0	0.8	1.6	1.0	0.4	0.4	3.5	0.6	0.4	0.7	0.5	0.3	0.2	0.1	0.7
PCB 105	5	0.2	0.2	0.5	0.4	0.1	0.1	1.1	0.2	0.1	0.2	0.2	0.1	0.1	0.0	0.1
PCB 126	5															
PCB 153	6	5.3	3.3	5.6	3.5	1.0	1.3	6.2	3.0	2.0	2.8	2.6	0.8	0.8	0.3	0.8
PCB 138	6	2.6	1.6	3.1	1.8	0.5	0.6	3.4	1.6	1.0	1.4	1.4	0.4	0.4	0.2	0.5
PCB 128	6	0.3	0.2	0.4	0.3	0.0	0.0	0.7	0.2	0.1	0.2	0.2	0.1	0.1	0.0	0.1
PCB 187	7	2.9	1.9	3.0	1.8	0.6	0.4	3.2	1.6	1.0	1.4	1.4	0.3	0.3	0.2	0.5
PCB 180	7	3.9	2.4	3.9	2.7	0.7	0.7	2.9	2.2	1.5	1.8	1.9	0.4	0.4	0.2	0.6
PCB 170	7	1.8	1.1	1.8	0.9	0.2	0.3	1.4	1.0	0.6	0.8	0.9	0.2	0.2	0.0	0.2
PCB 195	8								0.1	0.1						
PCB 206	9															
PCB 209	10															
PRC 32	3	3	2	16	2	5	3	8	3	2	5	5	2	4	5	14
PRC 54	4	2	5	20	1	8	4	14	2	3	7	7	2	6	7	26
PRC 47	4	38	48	66	50	76	59	196	38	55	72	66	59	71	69	92
PRC 101	5	34	43	65	45	116	58	149	34	65	63	71	69	76	70	73
PRC 111	5	22	55	76	55	426	52	110	22	57	44	62	69	66	63	51
PRC 138	6	21	40	65	52	190	50	111	21	58	43	60	70	61	59	45
PRC 178	7	15	38	67	49	432	42	91	15	45	31	46	59	50	50	33

Congener	# Cl	2017 0-5 cm PE						2017 WC PE				
		S1	S3	S4	S8	S9	S10	S1	S2	S4	S8	S10
PCB 8	2	1										
PCB 18	3	1	1	1	1		1	1			0.4	1
PCB 28	3	6	5	4	3	3	6	5		4	3	6
PCB 52	4	23	10	8	5	4	10	13	10	11	3	9
PCB 44	4	3	2	1	1	1	2	2	2	2	1	2
PCB 66	4	5	6	2	3	2	4	5	5	4	2	5
PCB 77	4							1				
PCB 101	5	13	11	10	8	5	8	11	10	12	4	8
PCB 118	5	4	5	3	4	2	5	4	5	4	2	6
PCB 105	5	1	2	1	2	1	2	2	2	1	1	2
PCB 126	5	4	3	3	2	1	1	5	3	3	1	2
PCB 153	6	27	24	20	16	7	11	24	20	22	6	12
PCB 138	6	14	21	16	7	5	10	12	10	20	3	8
PCB 128	6	2	2	2	1	1	1	2	2	1	0.4	1
PCB 187	7	10	8	8	5	2	3	10	7	8	2	6
PCB 180	7	14	11	115	7	3	3	14	10	11	3	8
PCB 170	7	7	6	5	3	1	2	7	5	6	2	4
PCB 195	8	1		1						1		1
PCB 206	9			0.3								0.5
PCB 209	10											0.3
PRC 32	3	1	1	1	1	1	1				0.5	2
PRC 54	4	0.1	1	0.5		1	1			1	0.03	1
PRC 47	4	8	1	8	7	14	25	4	5	8	11	10
PRC 101	5	10	2	8	11	11	21	12	15	18	22	21
PRC 111	5	12	3	9	12	8	18	25	28	32	37	36
PRC 138	6	13	4	10	15	9	24	29	31	37	40	39
PRC 178	7	14	4	10	14	7	14	38	41	47	49	69

Table S13 C_w, PRC estimated (pg PCB/L water)

Congener	# Cl	2016 0-5 cm PE water concentrations								2016 WC PE water concentrations						
		S1	S2	S2A	S3	S7	S8	S9	S10	S1	S2A	S2	S3	S8	S9	S10
PCB 8	2	-	-	-	-	-	-	-	-	-	-	-	-	-	-	-
PCB 18	3	6.7	18.1	10.2	4.9	-	-	20.3	6.5	9.1	6.6	7.2	5.1	3.9	3.6	5.9
PCB 28	3	12.7	35.5	12.3	11.2	7.3	6.1	30.6	8.6	12.2	12.9	11.0	7.4	7.1	4.4	8.9
PCB 52	4	53.2	79.0	31.5	38.7	15.6	15.7	81.4	38.8	40.2	35.9	38.9	16.9	13.6	10.1	20.9
PCB 44	4	10.8	12.6	13.4	10.2	4.7	5.3	17.8	7.0	7.9	7.8	6.9	4.0	3.5	2.4	4.5
PCB 66	4	11.7	12.9	11.2	9.5	5.2	4.8	17.8	5.2	6.2	7.1	6.5	3.6	3.6	2.5	3.7
PCB 77	4	-	-	-	-	-	-	-	-	-	-	-	-	-	-	-
PCB 101	5	37.2	32.4	27.8	20.8	11.9	13.9	39.8	17.3	16.8	20.8	16.5	11.2	8.7	7.1	16.9
PCB 118	5	11.3	9.7	10.6	7.9	4.0	3.7	21.5	4.8	4.6	6.9	4.7	2.9	2.6	2.3	7.7
PCB 105	5	1.7	1.9	3.3	2.8	1.0	0.9	7.0	1.5	1.4	1.8	1.6	0.9	0.8	0.5	1.2
PCB 126	5	-	-	-	-	-	-	-	-	-	0.1	-	-	-	-	-
PCB 153	6	63.3	42.9	36.9	26.8	10.9	11.3	38.3	26.2	22.0	30.1	24.2	8.6	8.7	6.0	8.7
PCB 138	6	31.0	20.2	20.6	13.7	6.3	5.6	21.5	13.7	11.3	15.4	13.0	4.9	4.6	3.4	5.9
PCB 128	6	4.2	2.5	3.0	2.1	-	-	4.4	1.8	1.6	2.0	1.8	0.8	0.8	0.7	1.1
PCB 187	7	25.7	17.8	14.6	10.3	4.9	2.4	14.8	10.5	7.9	10.7	9.6	2.8	2.6	2.2	3.6
PCB 180	7	35.6	23.5	19.9	15.6	6.0	4.8	13.8	14.5	12.1	14.6	13.7	3.9	3.3	2.8	4.5
PCB 170	7	16.6	10.6	9.1	5.6	1.9	2.1	6.8	6.7	4.9	6.3	6.2	1.7	1.5	0.7	2.0
PCB 195	8	-	-	-	-	-	-	-	0.8	0.9	0.1	0.1	-	-	-	-
PCB 206	9	-	-	-	-	-	-	-	-	-	0.1	-	-	-	-	-
PCB 209	10	-	-	-	-	-	-	-	-	-	0.1	-	-	-	-	-

Congener	# Cl	2017 0-5 cm PE water concentrations						2017 WC PE water concentrations				
		S1	S3	S4	S8	S9	S10	S1	S2	S4	S8	S10
PCB 8	2	7.1										
PCB 18	3	18.3	10.2	10.7	9.1	0.0	12.4	14.3			5.6	10.3
PCB 28	3	14.9	11.9	10.9	8.7	6.9	18.1	12.4		11.4	6.7	14.5
PCB 52	4	239.0	104.7	82.7	52.2	39.9	134.4	134.3	108.0	118.0	37.1	98.6
PCB 44	4	37.9	30.0	16.2	17.8	10.7	36.3	25.9	29.4	20.6	11.6	27.2
PCB 66	4	23.4	26.4	10.4	15.8	7.7	49.0	22.5	22.5	17.8	10.1	25.9
PCB 77	4								5.0			
PCB 101	5								62.6	86.0	35.7	73.2
PCB 118	5	29.1	21.4	18.8	29.0	12.7	128.4	24.1	28.7	26.6	17.3	52.3
PCB 105	5	7.9	7.3	5.5	10.9	3.3	46.0	8.5	10.7	8.4	6.8	18.2
PCB 126	5	31.8	14.0	21.1	16.6	5.8	40.3	29.3	23.0	26.1	10.2	19.5
PCB 153	6	302.7	120.3	176.4	182.6	59.7	654.2	218.7	213.5	298.0	98.4	221.9
PCB 138	6	161.2	125.4	152.2	79.5	52.1	592.2	122.3	111.5	286.0	47.8	145.4
PCB 128	6	21.6	12.5	17.2	19.0	6.4	65.3	18.7	20.5	20.4	7.0	25.4
PCB 187	7	109.2	40.0	68.3	58.7	16.9	150.5	87.0	74.5	104.0	38.4	106.1
PCB 180	7	398.4	120.5	2423.8	190.3	57.5	530.8	308.7	257.5	389.2	135.9	391.7
PCB 170	7	195.7	69.3	122.2	103.5	27.5	299.4	158.5	140.7	200.7	69.8	201.6
PCB 195	8	88.1		45.7						97.2		110.3
PCB 206	9			27.9								101.2
PCB 209	10											184.4

Table S14 Average C_{water} Site 1 (Pegan Cove) and Site 8 (South Pond)

Congener	# Cl	2016 0-5 cm				2016 WC				2017 0-5 cm				2017 WC		
		Site 1	SD	Site 8	SD	Site 1	SD	Site 8	SD	Site 1	SD	Site 8	SD	Site 1	SD	Site 8*
PCB 8	2									2.4	4.1			0.0		
PCB 18	3	10.0	5.8			7.3	1.2	4.2	0.8	13.1	4.5	4.5	6.4	4.8	8.3	5.6
PCB 28	3	17.9	13.8	6.7	0.8	11.2	1.9	6.3	1.7	12.6	2.1	7.8	1.3	7.9	6.9	6.7
PCB 52	4	50.6	38.0	15.7	0.1	38.5	1.8	13.5	3.4	142.1	84.6	46.1	8.6	120.1	13.2	37.1
PCB 44	4	11.8	7.4	5.0	0.4	7.4	0.5	3.3	0.8	28.0	11.0	14.3	5.0	25.3	4.4	11.6
PCB 66	4	11.3	7.4	5.0	0.3	6.3	0.8	3.2	0.7	20.1	8.5	11.7	5.7	20.9	2.7	10.1
PCB 77	4									0.0	0.0	0.0	0.0	1.7	2.9	0.0
PCB 101	5	29.5	15.6	12.9	1.4	17.8	2.0	9.0	2.0	65.5	17.2	40.6	16.8	70.6	13.3	35.7
PCB 118	5	9.9	10.2	3.8	0.2	5.3	1.1	2.6	0.3	23.1	5.4	20.9	11.6	26.5	2.3	17.3
PCB 105	5	2.4	3.5	0.9	0.1	1.6	0.2	0.7	0.2	6.9	1.3	7.1	5.3	9.2	1.3	6.8
PCB 126	5									22.3	9.0	11.2	7.6	26.1	3.1	10.2
PCB 153	6	42.5	15.7	11.1	0.3	25.6	3.5	7.8	1.5	199.8	93.5	121.2	86.9	243.4	47.4	98.4
PCB 138	6	21.4	9.0	5.9	0.5	13.4	1.7	4.3	0.8	146.3	18.6	65.8	19.4	173.3	97.8	47.8
PCB 128	6	3.0	2.5			1.8	0.2	0.8	0.1					19.9	1.0	7.0
PCB 187	7	17.1	6.5	3.7	1.8	9.7	1.3	2.5	0.3					88.5	14.8	38.4
PCB 180	7	23.7	4.9	5.4	0.9	13.7	1.2	3.3	0.5					318.5	66.4	135.9
PCB 170	7	10.5	2.8	2.0	0.1	6.0	0.8	1.3	0.5					166.6	30.8	69.8
PCB 195	8					0.5	0.4							32.4	56.1	
PCB 206	9					0.1										
PCB 209	10					0.1										

Only S8 measured in South Pond of 2017 WC

Table S15 C_{lipid} predicted from average C_{water}

Congener	# Cl	2016 0-5 cm				2016 WC				2017 0-5 cm				2017 WC		
		Site 1	SD	Site 8	SD	Site 1	SD	Site 8	SD	Site 1	SD	Site 8	SD	Site 1	SD	Site 8*
PCB 8	2					8.0				0	1					
PCB 18	3	12.2	7.1			9.0	1.5	5.1	1.0	11	4	4	5	4	7	5
PCB 28	3	11.2	8.7	4.2	0.5	7.0	1.2	3.9	1.0	5	1	3	1	3	3	3
PCB 52	4	198.6	149.0	61.5	0.3	151.0	7.1	53.1	13.5	334	199	108	20	282	31	87
PCB 44	4	47.3	29.8	20.0	1.7	29.7	2.0	13.4	3.2	66	26	34	12	60	10	27
PCB 66	4	61.6	40.1	27.1	1.5	34.0	4.4	17.5	3.6	63	27	37	18	66	8	32
PCB 77	4						0.0	0.0	0.0					4	6	
PCB 101	5	325.9	171.9	141.9	15.8	196.6	22.3	99.3	22.4	410	108	254	105	442	84	223
PCB 118	5	141.6	146.6	55.1	2.6	75.4	15.8	37.3	4.3	182	42	165	91	209	19	137
PCB 105	5	35.6	52.0	14.0	1.6	23.3	2.7	10.6	2.6	55	10	56	42	72	10	54
PCB 126	5									230	93	116	79	270	32	106
PCB 153	6	1315.1	487.5	343.1	8.7	793.3	107.4	241.7	47.5	3328	1557	2018	1448	4054	789	1640
PCB 138	6	681.4	287.1	188.8	15.0	425.8	53.4	136.9	24.1	2436	309	1095	323	2886	1628	796
PCB 128	6	97.3	83.5			59.3	5.9	24.6	2.4	285	76	212	149	331	16	117
PCB 187	7	577.4	221.2	124.1	59.3	327.2	43.5	86.1	11.2	1241	595	646	506	1514	253	658
PCB 180	7	2091.3	430.7	475.7	76.5	1214.6	103.5	296.0	47.9	43482	55735	5493	4161	14118	2944	6023
PCB 170	7	947.7	251.7	182.7	13.3	545.8	69.7	120.5	46.3	5721	2814	2903	2382	7387	1367	3093
PCB 195	8					180.1	146.8			8115	8017			5896	10212	
PCB 206	9					15.5	31.0			1807	3130					
PCB 209	10					42.2	84.5			0	1					